From the DEPARTMENT OF BIOSCIENCES AND NUTRITION
Karolinska Institutet, Stockholm, Sweden

ANALYSIS OF PHENOTYPE REVERSIBILITY IN HUTCHINSON-GILFORD PROGERIA SYNDROME IN MICE

Charlotte Strandgren

Stockholm 2017

Published by Karolinska Institutet.
Printed by E-Print AB 2017

ISBN 978-91-7676-647-7

Analysis of phenotype reversibility in Hutchinson-Gilford progeria syndrome in mice

THESIS FOR DOCTORAL DEGREE (Ph.D.)

By

Charlotte Strandgren

Principal Supervisor:
Associate Professor Maria Eriksson
Karolinska Institutet
Department of Biosciences and Nutrition

Co-supervisor:
Professor Ola Nilsson
Karolinska Institutet
Department of Women's and Children's Health
Örebro University
Department of Medical Sciences

Opponent:
Associate Professor Kan Cao
University of Maryland
Department of Cell Biology and Molecular Genetics

Examination Board:
Professor Göran Andersson
Karolinska Institutet
Department of Laboratory Medicine

Professor Einar Hallberg
Stockholm University
Department of Neurochemistry

Professor Thomas Nyström
University of Gothenburg
Department of Microbiology and Immunology

Dedicated to my beloved family:

My mother Barbro, my brother Daniel and my sister-in-heart Jenny

My husband Martin, our daughter Isabella and our unborn son

My beloved cat Busan, see you on the other side

I love you all

ABSTRACT

Aging affects all people and is a complex process involving both genetic and environmental factors in a way that is not yet completely understood. Studies of premature aging syndromes might be helpful to acquire further clues to understand the molecular mechanisms explaining how aging occurs. Hutchinson-Gilford progeria syndrome (HGPS or progeria) is a genetic disease causing segmental premature aging in children, with an approximated incidence of 1 in 20 million individuals. Children affected by progeria appear normal at birth, but they begin developing symptoms of disease within the first years of life. Symptoms of HGPS include severe growth retardation, scleroderma-like skin changes, bone and tooth abnormalities, and loss of hair and body fat. The children with progeria die prematurely at a median age of 14.6 years, due to complications from cardiovascular disease and atherosclerosis.

In **Paper I**, we demonstrated that an already developed HGPS bone disease phenotype to a large extent could be reversed in a mouse model. We also showed that the level of reversibility was dependent on timing, since earlier transgenic suppression resulted in a better recovery of the bone phenotype. When resveratrol was assessed as a treatment option, we could only find few beneficial effects of the treatment. Since the human skeleton is continuously remodeled, substantial skeletal improvements could be obtained if the progeria mutation could be suppressed in patients, giving hope for the future treatment of children with progeria.

In **Paper II**, we developed a conditional mouse model expressing the most common HGPS mutation in brain, and to a less extent also in bone, skin and heart. We showed that long-term expression of the HGPS mutation in the brain, with subsequent accumulation of progerin, resulted in severe neuronal distortions. Despite this, aged HGPS mice did not experience any neuropathological changes or alterations in gene expression. Hence, our results suggest that neuronal cells are less sensitive to the functional deleterious effects of progerin expression.

In **Paper III**, in order to gain deeper knowledge of how the teeth are affected in HGPS, we further characterized the mandibular molars of our bone-specific mouse model expressing the most common HGPS mutation in osteoblasts, osteocytes and odontoblasts. We show that progerin expression significantly disturbs secondary dentin formation and that excessive deposition of irregular tertiary dentin takes place. Our findings could be used to elucidate the mechanisms involved in formation of reparative tertiary dentin, which might be applicable in a clinical setting to stimulate tertiary dentin formation.

In **Paper IV**, the skeletal phenotype of a previously developed knock-in mouse model with systemic expression of progerin was characterized. Progeria mice showed a significantly higher frequency of empty osteocyte lacunae in cortical bone tissue as well as a higher incidence of ribcage calluses compared to wild-type mice. Bone marrow phenotyping showed that the mesenchymal stem cell population was impaired, and mesenchymal stem cells showed an increased adipogenic and osteogenic differentiation capacity compared to wild-type mice. Our results suggest that mesenchymal stem cell transplantation from healthy donors might be a treatment strategy for HGPS that could be tested in this mouse model.

LIST OF SCIENTIFIC PAPERS

I. **Transgene silencing of the Hutchinson-Gilford progeria syndrome mutation results in a reversible bone phenotype, whereas resveratrol treatment does not show overall beneficial effects**
Strandgren C, Nasser HA, McKenna T, Koskela A, Tuukkanen J, Ohlsson C, Rozell B, Eriksson M. *FASEB J*. 2015, 29: 3193-205

II. **Expression of progerin in aging mouse brains reveals structural nuclear abnormalities without detectible significant alterations in gene expression, hippocampal stem cells or behavior**
Baek JH, Schmidt E*, Viceconte N*, Strandgren C*, Pernold K, Richard TJ, Van Leeuwen FW, Dantuma NP, Damberg P, Hultenby K, Ulfhake B, Mugnaini E, Rozell B, Eriksson M. *Hum Mol Genet*. 2015, 24: 1305-21. *Equal contribution

III. **Expression of the Hutchinson-Gilford Progeria mutation disturbs secondary dentin formation but promotes tertiary dentin formation**
Kim TH*, Choi H*, Strandgren C, Eriksson M, Cho ES. *Manuscript submitted*. *Equal contribution

IV. **Phenotypic analysis of bone marrow from Hutchinson-Gilford progeria mice suggests a lower mesenchymal stem cell count**
Strandgren C, Xiao P, Revêchon G, Qian H, Eriksson M. *Manuscript*

CONTENTS

LIST OF ABBREVIATIONS

BrdU	5-Bromo-2-deoxyuridine
eGFP	Enhanced green fluorescent protein
FACS	Fluorescence-activated cell sorting
FTI	Farnesyltransferase inhibitor
HSC	Hematopoietic stem cell
HGPS	Hutchinson-Gilford progeria syndrome
ICMT	Isoprenylcystein carboxylmethyltransferase
iPSC	Induced pluripotent stem cell
IRES	Internal ribosomal entry site
LAP	Lamin associated protein
LINC	Lincer of nucleoskeleton and cytoskeleton
MSC	Mesenchymal stem cell
NPC	Nuclear pore complex
NSE-tTA	Neuron specific enolase tetracycline-controlled transactivator
OMIM	Online Mendelian Inheritance in Man
OBC	Osteoblast progenitor cell
PFA	Paraformaldehyde
PD	Postnatal day
Sp7-tTA	Osterix tetracycline-controlled transactivator
TRAP	Tartrate-resistant acid phosphatase
tTA	Tetracycline-controlled transactivator
WT	Wild-type

1 INTRODUCTION

Aging is a natural part of life, but when and how the different age-related symptoms appear is highly individual, which most likely is due to various genetic and environmental factors, ultimately telling us that aging is a very complex process. In general, aging is characterized by progressive functional decline and increased vulnerability to pathologies such as cancer, cardiovascular disease, diabetes, and neurodegenerative disorders, and in the end death (Lopez-Otin *et al.*, 2013). Nine different hallmarks of aging have been proposed and categorized into three different groups: (i) Primary hallmarks, causes of damage: genomic instability, telomere attrition, epigenetic alterations, and loss of proteostasis; (ii) Antagonistic hallmarks, responses to damage: deregulated nutrient sensing, mitochondrial dysfunction, and cellular senescence; and (iii) Integrative hallmarks, cause of the phenotype: stem cell exhaustion and altered intercellular communication (Lopez-Otin *et al.*, 2013). The interactions of the molecular mechanisms causing aging are not completely understood, therefore further research is needed in order to increase the knowledge base and improve health and life quality. One way to study aging is through progeroid syndromes, such as the premature aging disease Hutchinson-Gilford progeria syndrome. Connections between progeroid diseases and regular aging may increase the understanding of the molecular mechanisms underlying aging.

1.1 HUTCHINSON-GILFORD PROGERIA SYNDROME

Hutchinson-Gilford progeria syndrome, also referred to as HGPS or progeria (Online Mendelian Inheritance in Man (OMIM), #176670), is a very rare genetic disease characterized by multiple features of premature/accelerated aging in children. Progeria was first described by Jonathan Hutchinson in 1886 and by Hastings Gilford in 1897 (Hutchinson, 1886; Gilford, 1897), but it took more than a century before the genetic cause for HGPS was finally uncovered in 2003 (De Sandre-Giovannoli *et al.*, 2003; Eriksson *et al.*, 2003), a *de novo* single point mutation in exon 11 of the *LMNA* gene (c.1824C>T, p.G608G). The mutation, accounting for the great majority of progeria cases, is silent and does not change the amino acid sequence of that codon, however, it results in the increased activation of a cryptic splice site and the generation of a truncated form of lamin A commonly called progerin or lamin AΔ50 (De Sandre-Giovannoli *et al.*, 2003; Eriksson *et al.*, 2003). HGPS affects approximately 1 in 20 million individuals, and affected children have been found all over the world seemingly without geographical bias (Gordon, 2016).

While children with progeria display no clinical signs of disease at birth, the disease usually presents within their first years of life when they gradually develop an appearance often referred to as aged-like. Progeria is clinically manifested as severe growth retardation, scleroderma-like skin changes, alopecia, loss of subcutaneous adipose tissue, skeletal dysplasia, joint stiffness, abnormal and delayed dentition, and atherosclerosis with cardiovascular decline (Table 1) (DeBusk, 1972; Hennekam, 2006; Gordon *et al.*, 2007;

Merideth *et al.*, 2008; Gordon *et al.*, 2011). Death occurs prematurely, where the median age of survival 14.6 years, and the most common causes of death are due to complications from cardiovascular disease and atherosclerosis (Merideth *et al.*, 2008; Gordon *et al.*, 2014a). Even though the expression pattern for lamin A includes all terminally differentiated cells and tissues (Stuurman *et al.*, 1998), age-associated features like cancer, cataract, Alzheimer, and senility are absent among the clinical symptoms in HGPS and the children show no defects in their mental and intellectual abilities (Table 1) (Hennekam, 2006; Merideth *et al.*, 2008). And, despite the presence of multiple premature aging symptoms, several other organs also seem to be completely unaffected, such as the liver, kidneys, lungs, bone marrow and gastrointestinal tract (Kieran *et al.*, 2007).

Table 1. Clinical manifestations of Hutchinson-Gilford progeria syndrome (Merideth *et al.*, 2008) in comparison to regular aging.

Clinical symptoms	HGPS	Regular aging
Abnormal and delayed dentition	✓	
Alopecia	✓	✓
Atherosclerosis	✓	✓
Cancer		✓
Cardiovascular disease and stroke	✓	✓
Growth retardation	✓	
Joint stiffness	✓	✓
Loss of subcutaneous adipose tissue	✓	✓
Neurodegeneration		✓
Reduced bone mineral density	✓	✓
Scleroderma-like skin changes	✓	
Skeletal dysplasia	✓	
Vascular calcification	✓	✓

1.2 LAMINS AND THE *LMNA* GENE

Lamins are type V intermediate filament proteins that polymerize into tetrameric filaments and are the main components of the lamina network, which underlies the inner nuclear membrane (Turgay *et al.*, 2017). Lamins can also be found throughout the nucleoplasm, and in proliferating cells the nucleoplasmic pool of lamin A/C accounts for 10-15% of the total amount of lamin A/C (Dechat *et al.*, 2008; Kolb *et al.*, 2011). The nucleoplasmic lamin A/C is more dynamic and less tightly bound to the nucleoskeleton compared to the peripheral counterparts (Dechat *et al.*, 2008). There are two types of lamins: A- and B-type. A-type lamins are all encoded by the *LMNA* gene, which consists of 12 exons and is located on chromosome 1q22. De different A-type lamins are produced by alternative splicing, where the two major isoforms are lamin A (exon 1-12) and lamin C (exon 1-10) (Figure 1), and the minor isoforms are lamin AΔ10, lamin AΔ50, and lamin C2 (Fisher *et al.*, 1986; Machiels *et al.*, 1996). The B-type lamins contain the two major proteins lamin B1, encoded by the

LMNB1 gene, and lamin B2, encoded by the *LMNB2* gene. The B-type lamins also contain the minor isoform lamin B3, which is also encoded by the *LMNB2* gene (Dechat *et al.*, 2010). A-type lamins are expressed in more differentiated cells (Rober *et al.*, 1989), while the B-type lamins can be found in all cells and are also expressed throughout development. The lamin proteins are composed of a long central α-helical rod domain, which is flanked by globular N-terminal (head) and C-terminal (tail) domains (Figure 1) (Fisher *et al.*, 1986).

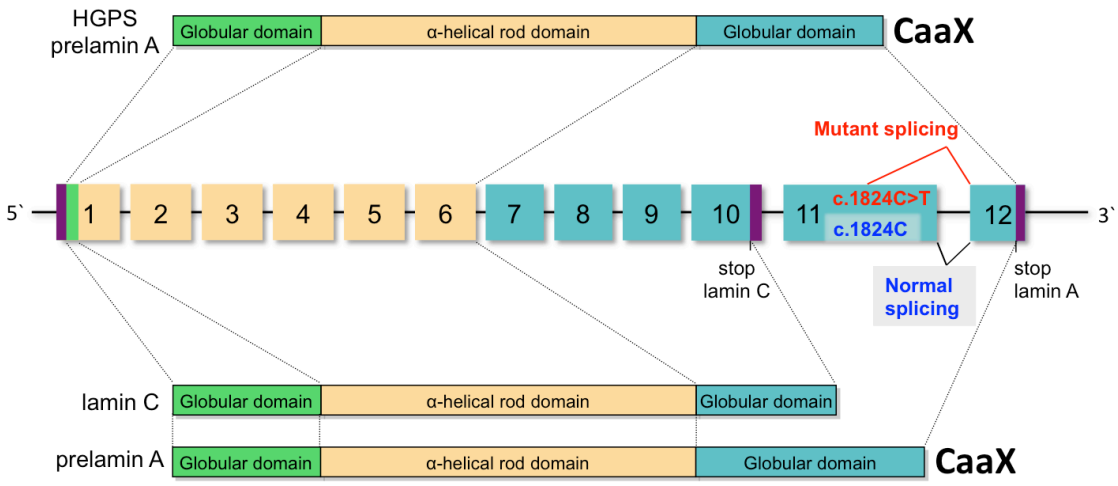

Figure 1. The *LMNA* gene. Schematic drawing of the *LMNA* gene and the normal splicing protein products lamin C and prelamin A. The most common HGPS mutation, c.1824C>T, is also shown and the following mutant splicing, resulting in the truncated HGPS prelamin A protein product. Not to scale. The drawing was inspired by (Capell and Collins, 2006).

1.2.1 Post-translational processing of prelamin A

Production of the mature lamin A protein requires a series of processing steps of the prelamin A precursor protein (Figure 2) (Sinensky *et al.*, 1994). Prelamin A terminates with at CAAX motif (-CSIM) that acts as a target for the first processing step, farnesylation, when a farnesyl lipid is attached to the cysteine residue by farnesyltransferase (FTase). Secondly, the –AAX motif is cleaved off by either ZMPSTE24 or RCE1. The third processing step involves carboxylmethylation of the newly exposed C-terminal cystein by isoprenylcystein carboxylmethyltransferase (ICMT). The final step entails the cleavage of the 15 terminal amino acids by ZMPSTE24, including the farnesylated cysteine-methyl residue, producing the mature lamin A protein (Young *et al.*, 2006).

The underlying genetic defect for classical HGPS, the c.1824C>T (p.G608G) mutation in exon 11 of the *LMNA* gene, results in an increased activation of a cryptic splice site and the generation of a truncated form of prelamin A with a 50-amino-acid internal deletion (De Sandre-Giovannoli *et al.*, 2003; Eriksson *et al.*, 2003). Through this internal deletion, several phosphorylation sites in addition to the RSYLLG motif, used as a recognition site for the

final cleavage by ZMPSTE24, has been removed from the prelamin A precursor protein, resulting in failure of the terminal cleavage step (Figure 2). Thus, the end product is an only partially processed lamin A protein that remains permanently farnesylated (Dechat *et al.*, 2007), and is referred to as progerin. In HGPS cells though, both normal lamin A and the immature progerin protein are produced.

It has been shown that progerin levels accumulate with increased age, likely being the cause of the progressive nature of the disease (Goldman *et al.*, 2004; Rodriguez *et al.*, 2009). Progerin has also been found at lower levels in cells from normal unaffected individuals (Scaffidi and Misteli, 2006; Cao *et al.*, 2007). As in HGPS, the levels of progerin have been discovered to increase with cellular aging in unaffected cells, supporting the hypothesis of a common underlying mechanism for HGPS and normal aging (Cao *et al.*, 2007; Rodriguez *et al.*, 2009). It has also been shown that progressive telomere shortening during cellular senescence induced progerin production in normal human fibroblasts (Cao *et al.*, 2011a).

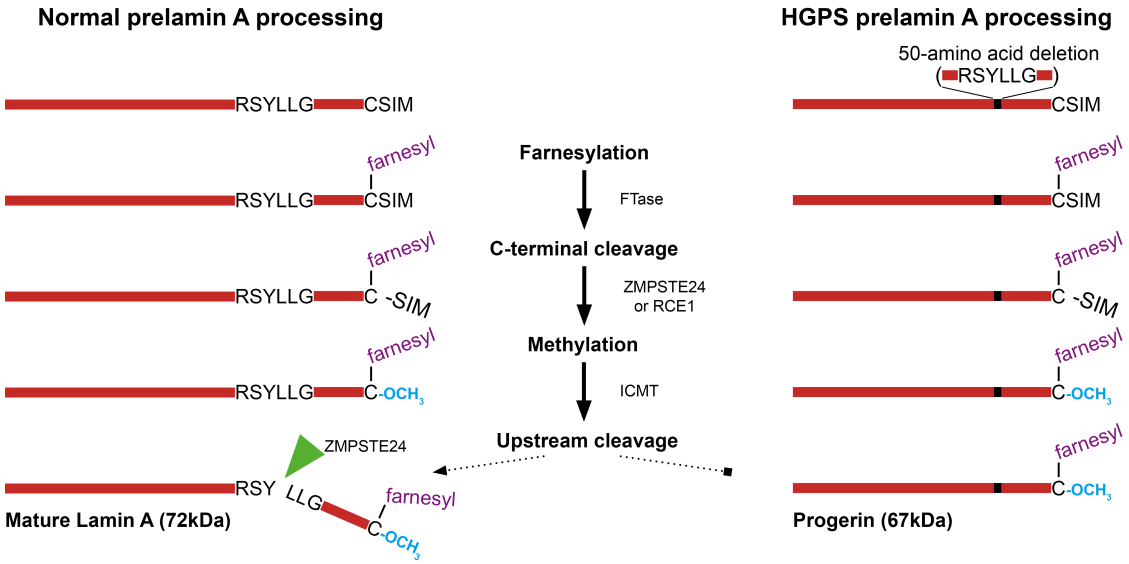

Figure 2. The post-translational processing of prelamin A. Schematic drawing of the post-translational modifications steps of normal prelamin A and in HGPS. The production of mature lamin A involves multiple steps (left). In HGPS, the recognition site (RSYLLG) for the final cleavage by ZMPSTE24 is missing due to the 50-amino-acid deletion (right). Hence, the final processing step cannot take place, resulting in a permanently farnesylated and carboxylmetylated truncated prelamin A protein known as progerin. Not to scale. The drawing was inspired by (Young *et al.*, 2006).

1.3 THE NUCLEAR LAMINA

The nuclear envelope separates the cell nucleus from the cytoplasm, and it is composed of three major components: (i) the outer and inner nuclear membrane; (ii) the nuclear pore complexes; and (iii) the nuclear lamina (Figure 3) (Stuurman *et al.*, 1998). The outer nuclear membrane is connected to the rough endoplasmatic reticulum, and also contains numerous protein producing ribosomes. The inner nuclear membrane has a different set of membrane proteins, it is not known to participate in protein synthesis, and is closely associated with the nuclear lamina and underlying chromatin (reviewed by Burke and Stewart, 2002). The outer and inner nuclear membranes are connected through the nuclear pore complexes (NPC), which are large macromolecular complexes forming channels across the nuclear envelope, mediating the bidirectional nucleo/cytoplasmic transport of proteins and RNA (Stuurman *et al.*, 1998; Burke and Stewart, 2002).

The nuclear lamina is located underneath the inner nuclear membrane, and it is a filamentous meshwork composed of A- and B-type lamins and nuclear lamin-associated membrane proteins (Figure 3). The nuclear lamina determines the shape and size of the cell nucleus, is involved in DNA replication and transcription, and it also anchors the chromatin and assures correct localization of the NPCs in the nuclear envelope (Stuurman *et al.*, 1998; Moir and Spann, 2001; Burke and Stewart, 2002; Dechat *et al.*, 2008). The nuclear lamina also provides mechanical support and mechanochemical properties of the nucleus, where A-type lamins are accountable for the nuclear stiffness and viscosity, and B-type lamins provide nuclear elasticity (Swift *et al.*, 2013).

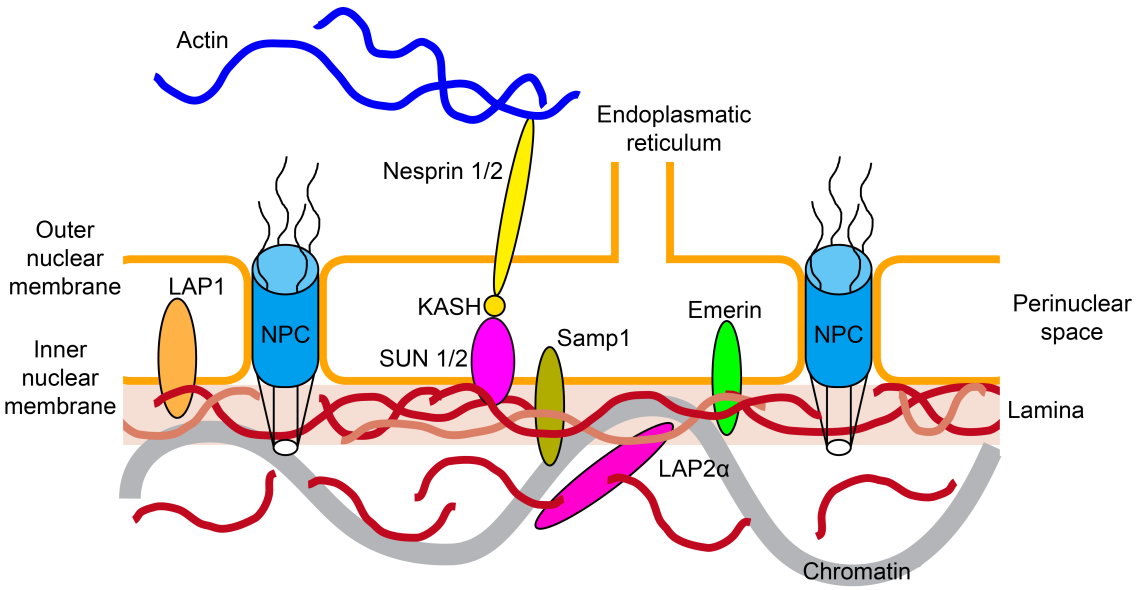

Figure 3. The nuclear envelope. Schematic drawing showing the nuclear envelope, a selection of known lamin-associated membrane proteins and the nuclear lamina, which is located underneath the inner nuclear membrane. The lamina provides nuclear stability, anchors chromatin and assures correct localization of the nuclear pore complexes (NPC). The lamina interacts with the cytoskeleton (actin) through the LINC complex (SUN 1/2 connects to Nesprin 1/2 via their KASH domain). Not to scale. The drawing was inspired by (Goldman *et al.*, 2002; Burke and Stewart, 2006).

Studies have identified the nuclear lamins to interact with a great number of proteins in the inner nuclear membrane and the nucleoplasm, some of which are lamina-associated polypeptides (LAP1 and LAP2α) (Foisner and Gerace, 1993; Dechat *et al.*, 2000), emerin (Clements *et al.*, 2000), the SUN proteins (SUN1 and 2) (Crisp *et al.*, 2006), and Samp1 (Gudise *et al.*, 2011). In a recent study it was found that the expression of inner nuclear membrane proteins was differentially and developmentally dynamic and showed high cell type specificity, and they identified that the inner nuclear membrane protein LEMD2 (LAP2/emerin/MAN1 domain-containing protein 2) was specifically interacting with A-type lamins (Thanisch *et al.*, 2017). LAP2α is localized in the nucleoplasm, where it interacts with and stabilizes the nucleoplasmic lamin A/C (Dechat *et al.*, 2000), and these complexes have been associated with regulation of cell proliferation, differentiation of progenitor cells and chromatin organization (Vidak and Foisner, 2016). Emerin is located in the inner nuclear membrane, where it interacts with lamin A (Clements *et al.*, 2000). The main mediator of mechanical force transmission from the cytoskeleton into the nucleus is however the LINC complex (linker of nucleoskeleton and cytoskeleton). The LINC complex consists of the lamina interacting SUN proteins, spanning the inner nuclear membrane, that in the perinuclear space are connected to nesprins 1 and 2 (nuclear envelope spectrin repeat proteins), which are KASH domain proteins located in the outer nuclear membrane (Crisp *et al.*, 2006). The nesprins are in turn connected to actin, thereby allowing force transmission from the extracellular matrix via the cytoskeleton and into the nucleus, contributing to mechanosignal transduction (Lombardi *et al.*, 2011). Samp1 is located in the inner nuclear membrane and has been shown to interact with the A-type lamina network, and to partially co-localize with the LINC complex protein SUN1 (Gudise *et al.*, 2011). Resent studies have indicated that lamin A levels increase in response to force, and also affects the cell fate and differentiation where increased lamin A levels result in differentiation into a stiffer tissue (Swift *et al.*, 2013).

1.3.1 Cellular phenotype in HGPS

In HGPS, the farnesylation of progerin enables the protein to stay more tightly associated with the inner nuclear membrane, causing major impairment of the structure of the nucleus with blebbing of the nuclear envelope, thickened nuclear lamina, mislocalization and clustering of NPCs, and loss of heterochromatin anchoring (Table 2) (Goldman *et al.*, 2004; Vidak and Foisner, 2016). In addition, the expression of progerin has been shown to cause epigenetic changes and genomic damage (Gordon *et al.*, 2014b), as well as mitochondrial morphological and behavior defects (Xiong *et al.*, 2016). One example of progerin associated genomic damage was shown in a recent study, where progerin accumulation in HGPS vascular smooth muscle cells caused down-regulation of PARP1, an essential molecular switch having dual roles: (i) sensing and initiating repair of DNA single-strand breaks; and (ii) suppressing error-prone non-homologous end joining and instead favoring repair by homologous recombination upon DNA double-strand breaks. The progerin mediated

suppression of PARP1 activated non-homologous end joining response, leading to error-prone DNA repair, which resulted in chromosome aberrations, mitotic catastrophe and subsequent cell death (Zhang *et al.*, 2014). This study shows a molecular pathway causing the progressive loss of vascular smooth muscle cells in HGPS. In another recent study, it was shown that progerin impairs the NRF2 pathway (by sequestering of NRF2 that causes its mislocalization). Reactivation of NRF2 activity in cells from HGPS patients reversed the progerin-associated nuclear aging defects, as well as restored *in vivo* viability of MSCs in an animal model (Kubben *et al.*, 2016).

Table 2. Cellular phenotypes in Hutchinson-Gilford progeria syndrome. (Capell and Collins, 2006)

Cellular phenotypes in HGPS
Epigenetic changes
Genomic damage
Loss of heterochromatin anchoring
Mislocalization of nuclear pore complexes
Mitochondrial morphological and behavior defects
Nuclear blebbing
Thickened nuclear lamina

In normal healthy cells, the nuclei respond to shearing stress by re-distributing and up-regulating lamin A, which in HGPS does not work properly since progerin immobilizes lamin A in the lamina. Having this ability is crucial in tissues that are under a lot of mechanical stress, such as vasculature, bone and joints, which also happen to be tissues presenting some of the most prominent pathologies in HGPS (Swift *et al.*, 2013; Gordon *et al.*, 2014b). Progerin expression has also been shown to cause disturbances in the LINC complex by reducing SUN1 mobility (Chen *et al.*, 2014). The LINC complex is necessary for mechanosignaling and nucleocytoskeletal coupling, and impairment of this complex may further add to the reduced response capacity to shear stress in HGPS cells.

1.4 MESENCHYMAL STEM CELLS

Mesenchymal stem cells (MSCs) are multipotent stromal cells that are located in many tissues, such as bone marrow, adipose tissue, blood, skin and skeletal muscle, and they are able to differentiate into various cell types including myocytes, chondrocytes, adipocytes, fibroblasts and osteoblasts (Makino *et al.*, 1999; Pittenger *et al.*, 1999; Dezawa *et al.*, 2005). Exogenously administered MSCs have been shown to migrate to damaged tissues and participate in tissue repair, hence the potential of MSCs as a treatment for various diseases have been proposed (Liechty *et al.*, 2000; Devine *et al.*, 2003; Chan *et al.*, 2007; Guillot *et*

al., 2008). Transplantation of MSCs has also been used in many preclinical models of different diseases, including the treatment of myocardial infarction, rheumatoid arthritis, and acute renal failure (Uccelli *et al.*, 2008). In addition, promising results have also been shown in studies where MSCs were used to treat children with osteogenesis imperfecta (OI), which is a genetic disease caused by a mutation in one of the type I collagen genes, making the patient susceptible to bone breaks (Horwitz *et al.*, 1999; Horwitz *et al.*, 2001). However, while the clinical effect of MSC transplantation was not permanent, regular yearly infusions showed successful results in the clinical trials for OI, and only a few unfavorable effects could be attributed to MSC administration, emphasizing the therapeutic potential of this method (Horwitz *et al.*, 2002).

In HGPS, the majority of the affected tissues are of mesenchymal origin. It has recently been shown that MSCs, originating from induced pluripotent stem cells (iPSCs) from a progeria patient, express high levels of progerin (Zhang *et al.*, 2011). In addition, *in vitro* studies have shown that progerin interferes with proliferation and differentiation of MSCs (Scaffidi and Misteli, 2008; Zhang *et al.*, 2011; Xiong *et al.*, 2013).

1.5 BONE DEVELOPMENT AND REMODELING

The skeleton is a dynamic and metabolically active organ with many functions, which include providing shape, support, protection, storage of minerals, blood formation (hematopoiesis), and together with muscles and tendons it forms musculoskeletal systems that enables movement. The skeleton is primarily formed by cartilage and bone tissue, and it is a metabolically active organ that produces many paracrine and hormonal factors, but is regulated by both local factors and hormones travelling through the bloodstream to control bone development as well as bone remodeling during life (Kronenberg, 2003).

Formation of bone is initiated when mesenchymal cells starts forming condensations, which are cell clusters that adhere together through expression of adhesion molecules (Figure 4A). The mammalian osseous tissues are formed during embryogenesis by two different processes: intramembranous and endochondral bone formation, respectively. In intramembranous bone formation, condensed mesenchymal cells directly differentiate into bone-forming osteoblasts, laying down a type I collagen rich bone matrix. Many of the craniofacial flat bones are formed through this process. (Kronenberg, 2003; Long and Ornitz, 2013)

However, most of the bones, including the long bone and the vertebrae, are formed by endochondral bone formation, which generates bone via a cartilage intermediate stage. In this process, following the mesenchymal condensation, the cells in the core of the condensation differentiate into chondrocytes (Figure 4B) that secrete a matrix rich in type II collagen and proteoglycans, including aggrecan. The cells at the border of the condensation form the perichondrium and periosteum, which express type I collagen and separates the developing bone from its surroundings. After initial cartilage formation, the chondrocytes rapidly proliferate and produce more cartilage matrix, driving the growth of the forming bone. The

chondrocytes at the center then stop proliferating and enlarge into hypertrophic chondrocytes. Hypertrophic chondrocytes secrete a matrix rich in collagen type X (Figure 4C) (Kronenberg, 2003; Long and Ornitz, 2013). The hypertrophic chondrocytes couple chondrogenesis and osteogenesis by mineralization of their surrounding matrix, and by producing factors, including VEGF, that attracts the invading blood vessels and chondroclasts (Gerber *et al.*, 1999; Kronenberg, 2003). They also, by secreting Indian hedgehog, direct the neighboring perichondrial cells to differentiate into osteoblasts, which secrete bone matrix to form the bone collar (Figure 4D) (Chung *et al.*, 2001). The hypertrophic chondrocytes subsequently undergo apoptosis, and the cartilage matrix left behind acts as a scaffold for the invading osteoblasts and blood vessels (Kronenberg, 2003; Long and Ornitz, 2013). The vascular invasion leads to degradation of the cartilage, formation of the marrow, and deposition of bone matrix within the marrow cavity (Figure 4E) (Long and Ornitz, 2013). The bone matrix laid down by the osteoblasts creates the primary ossification center, which will generate the trabecular bone (Kronenberg, 2003; Long and Ornitz, 2013).

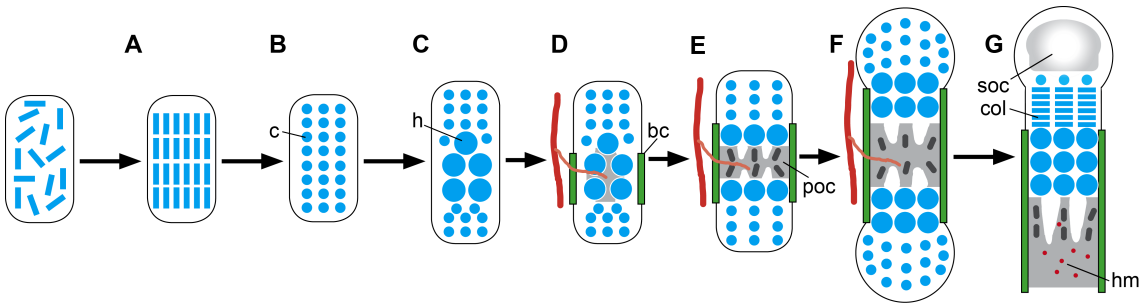

Figure 4. Endochondral bone formation. (A) Endochondral bone formation starts with formation of mesenchymal condensations. **(B)** Condensed cells differentiatie into chondrocytes (c). **(C)** Central chondrocytes stop proliferating and become hypertrophic (h). **(D)** Hypertrophic chondrocytes direct mineralization and attract blood vessels. Adjacent perichondrial cells become osteoblasts, forming the bone collar (bc). **(E)** Hypertrophic chondrocytes undergo apoptosis. The bone matrix laid down by osteoblasts creates the primary ossification center (poc). **(F)** Continued chondrocyte proliferation lengthens the bone. **(G)** Secondary ossification centers (soc) are formed at the ends of the bone as chondrocytes stop proliferating, get hypertrophic and promote vascular and osteoblast invasion. In the growth plate, proliferating chondrocytes forms ordered columns (col) directing the lengthening of the bone. Hematopoietic marrow (hm) expands in the marrow space. Not to scale. The drawing was inspired by (Kronenberg, 2003).

Alongside the differentiation and subsequent calcification occurring in the center, further lengthening of the forming bone has taken place through continued proliferation, hypertrophy, and matrix production of chondrocytes at the ends of the bone (epiphysis) (Figure 4F). As the bone expands, a portion of these chondrocytes become flattened and form columns that direct the lengthening of the bone (Figure 4G). Subsequently, a secondary ossification center is formed in the epiphysis. In the long bones of the limb, chondrogenesis proceeds between the primary and secondary ossification centres. This portion of cartilage is then known as the growth plate. The round chondrocytes at the top of the growth plate are termed resting chondrocytes since they no longer proliferate rapidly, and they serve as

precursors to the flat proliferating columnar chondrocytes (Abad *et al.*, 2002). The continuous proliferation of chondrocytes, their subsequent hypertrophy and ultimate replacement by newly formed trabecular bone at the diaphyseal side of the growth plate, results in distal movement of the growth plate and longitudinal growth of the bone (Long and Ornitz, 2013). Below the growth plate, hematopoietic marrow and stromal cells expands in the marrow space (Kronenberg, 2003). Interestingly, lineage-tracing studies suggest that growth plate chondrocytes may trans-differentiate into osteoblasts and other skeletal cells, and thereby make a significant contribution to the pool of skeletal and non-skeletal cells of the bone (Ono *et al.*, 2014).

In order to maintain the skeleton and ensure a healthy function with proper mechanical properties, the bone tissue is constantly being remodeled throughout life by the activities of the bone resorbing osteoclasts and bone forming osteoblasts. Imbalance between bone formation and bone resorption can result in both too little bone, as in osteoporosis, or too much bone tissue (osteoscleroris). (Alford *et al.*, 2015)

1.5.1 The osteocyte

For a long time it has been known that osteocytes are derived from osteoblasts, hence descending from MSCs. By the end of the bone formation phase, the matrix-producing osteoblast can continue in different developmental directions: (i) become an osteocyte; (ii) become a bone lining cell; or (iii) undergo programmed cell death (Dallas and Bonewald, 2010; Bonewald, 2011; Alford *et al.*, 2015).

By definition, an osteocyte is an osteoblast that has become embedded within the bone matrix. In the adult skeleton, osteocytes constitute 90-95% of all bone cells, and they can live up to decades within their lacunae in the bone tissue, hence being the longest-lived of the bone cells (Bonewald and Johnson, 2008; Bonewald, 2011). Osteocytes are commonly distributed regularly throughout the bone, and they are connected to each other and to the cells on the bone surface by an intercellular system of small canaliculi canals, allowing them to send signals of bone resorption or formation in response to mechanical strain (Bonewald and Johnson, 2008; Dallas and Bonewald, 2010). In addition, the canaliculi system also connects the osteocytes to the bone marrow, giving them the possibility to recruit osteoclasts to promote bone resorption and to regulate differentiation of MSCs (Bonewald and Johnson, 2008).

With increased age, the osteocytes eventually die and leave behind empty lacunae. In aged bone, the empty lacunae are associated with a reduced bone remodeling capacity. Osteocyte cell death can also occur in connection to pathological conditions, such as osteoarthritis and osteoporosis, ultimately resulting in increased fragility of the skeleton. Fragility like this is generally considered as a result of lost osteocyte capacity to sense micro-damage and/or a loss of ability to signal the need for skeletal reparation. Hence, osteocyte viability and

function plays a significant role in maintaining bone remodeling homeostasis and bone integrity. (Bonewald, 2011)

1.6 CONDITIONAL MOUSE MODELS FOR HGPS

In order to study the segmental nature of HGPS, two different mouse models with tetracycline-controlled progerin expression was used in this thesis (Papers I-III). Tetracycline inducible systems (Tet-system) are binary transgenic model systems allowing both spatial and temporal regulation of target genes. By using a tissue specific promoter, it is possible to express a target gene in a restricted area of the mouse, and adding or removing the tetracycline derivate (doxycycline, Dox) gives the possibility to regulate at which time points the target gene is expressed (Gossen and Bujard, 1992; Zhu *et al.*, 2002). By using this type of binary transgenic mouse model system, it is not only possible to study the effects of transgene expression in a specific tissue, but it is also gives the opportunity to study the possibility for disease reversal by first expressing a disease causing gene until a phenotype has been developed and then silencing that same gene.

1.6.1 The Tet-system

The Tet-system consists of two parts: the regulatory part and the response part. The regulatory part contains a tissue specific promoter that controls the expression of the regulatory element, which can either be a tetracycline-controlled transactivator protein (tTA) or a reverse tTA protein (rtTA). The response part consists of the target gene under the control of a tet operator (tetop), which will promote transcription of the downstream target gene in the presence of the tTA/rtTA protein (Figure 5). (Gossen and Bujard, 1992; Zhu *et al.*, 2002)

Systems using tTA are called Tet-Off, and systems using rtTA are called Tet-On. In the Tet-Off system, the absence of a tetracycline derivate (Dox) will promote binding of tTA to the tetop element, which will initiate transcription of the target gene (Figure 5A). In contrast, when Dox is present the tTA is prevented from binding to the tetop element due to conformational changes, inhibiting gene transcription (Figure 5A). The Tet-On system on the other hand works through an opposite mechanism, where absence of Dox inhibits target gene transcription and presence of Dox promotes transcription (Figure 5B). (Gossen and Bujard, 1992; Zhu *et al.*, 2002)

We have used the Tet-Off system in Papers I, II and III. In order to study the effects of progerin expression in the bone tissue, the Sp7 (osterix) promoter was used in Papers I and III, and to study the effects of long-term progerin expression in the brain the NSE (neuron specific enolase) promoter was used in Paper II.

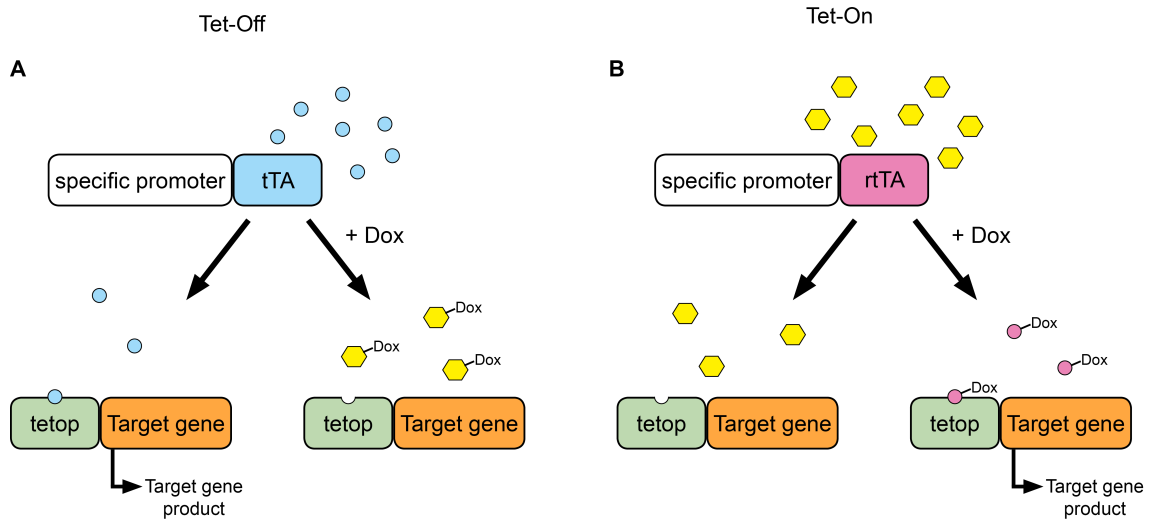

Figure 5. The Tet-Off and Tet-On systems. Schematic drawings of the Tet-Off **(A)** and Tet-On **(B)** systems, in which expression of the target gene is controlled by administration of doxycycline (Dox). **(A)** Induction of target gene expression in the absence of Dox. **(B)** Induction of target gene expression in the presence of Dox. Not to scale. The drawing was inspired by (Gossen and Bujard, 1992; Zhu *et al.*, 2002).

1.6.2 The minigene

To study the effects of progerin expression in specific tissues using the Tet-system, a minigene of human lamin A under the control of a tetop element has been developed (tetop-LA^{G608G}) (Sagelius *et al.*, 2008a). The minigene consists of exons 1-10, exon 11 (carrying the most common HGPS mutation, c.1824C>T, p.G608G), intron 11 and exon 12 from the human *LMNA* gene, followed by an internal ribosomal entry site (IRES) element, the coding region for enhanced green fluorescent protein (eGFP), and it ends with a SV40/polyA tail (Figure 6) (Sagelius *et al.*, 2008a). The IRES element allows for eGFP to be translated independently, and the SV40/polyA tail assists in nuclear export, translation and mRNA stability. The protein products generated from transcription of this minigene are human lamin A, progerin and eGFP.

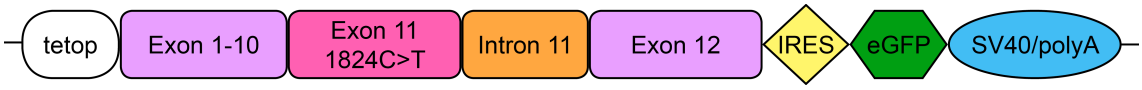

Figure 6. The minigene, tetop-LA^{G608G}. Schematic drawing of the minigene construct used for tissue specific expression of the most common HGPS mutation, c.1824C>T (tetop-LA^{G608G}). Transcription of the minigene generates human lamin A, progerin and eGFP. IRES, internal ribosomal entry site; eGFP, enhanced green fluorescent protein. Not to scale. The drawing was inspired by (Sagelius *et al.*, 2008a).

1.7 TREATMENT STRATEGIES FOR HGPS

Several attempts have been made to treat HGPS, both in progeria patient cell lines and in mouse models, where the treatment strategies generally have been to either directly target the mutation, the different lamin A post-translational processing steps, or progerin function and turnover. Here a selection of potential treatment strategies for HGPS has been reviewed (Table 3).

Since progerin has been shown to remain permanently farnesylated, an obvious candidate drug for treatment of HGPS would be farnesyltransferase inhibitors (FTIs), which work by inhibiting the farnesylation of the prelamin A precursor protein. Previous *in vitro* studies using HGPS patient cell lines, as well as cells from progeroid mice, showed vast improvements in the nuclear morphology (Capell *et al.*, 2005; Glynn and Glover, 2005; Toth *et al.*, 2005; Yang *et al.*, 2005). *In vivo* studies using two different HGPS mouse models and zmpste24-deficient mice also showed improved disease symptoms after treatment with FTIs (Fong *et al.*, 2006; Yang *et al.*, 2006; Capell *et al.*, 2008; Yang *et al.*, 2008).

Although treatment with FTIs inhibits prelamin A farnesylation, an *in vitro* study showed that an alternative pathway (via geranylgeranyltransferase) allowed for prelamin A processing in HGPS patient fibroblasts despite the usage of FTIs (Varela *et al.*, 2008). The same study also showed that a combination of statins and bisphosphonates inhibited both farnesylation and geranylgeranylation. This treatment improved the nuclear morphology in HGPS patient cell lines, as well as provided significant phenotype improvements in a zmpste24-deficient mouse model (Varela *et al.*, 2008)

Based on the positive outcomes from these studies two clinical trials have been performed in children with HGPS. Although some measures came out positive, including slight improvements in estimated lifespan, weight gain and reduction of vascular stiffness in many of the patients, the total improvements were limited, suggesting that there is still a need to evaluate other methods of treatment. (Gordon *et al.*, 2012; Gordon *et al.*, 2014a; Gordon *et al.*, 2016)

Another potential treatment target for HGPS that has been studied is the enzyme ICMT, which is also involved in the post-translational processing of prelamin A. A recent study using zmpste24-deficient mice showed beneficial results after inhibiting ICMT (Ibrahim *et al.*, 2013). In a stem cell transplantation study using another progeroid mouse model, having dysfunctional muscle-derived stem/progenitor cells, functional wild-type stem/progenitor cells isolated from the skeletal muscle of young mice were transplanted into the progeroid mice, resulting in significant lifespan and health span extension (Lavasani *et al.*, 2012).

Cells from HGPS patients have been successfully treated with the macrolide antibiotic drug rapamycin, showing abolished nuclear blebbing, enhanced progerin degradation, autophagy-mediated clearance of progerin, and delayed onset of cellular senescence (Cao *et al.*, 2011b). A recently published study using temsirolimus, a rapamycin analog with a more favorable pharmacokinetic profile than rapamycin, also showed beneficial effects in treatments of

Table 3. Selection of potential treatment strategies for Hutchinson-Gilford progeria syndrome and their effects following *in vitro* or *in vivo* treatments in relevant models.

Treatment / Drug	Pathway	Target	Evidence	Improvement(s)	Reference(s)
Bisphosphonates + statins*	geranyl-geranylation	prelamin A farnesylation	*in vitro* in patient cells	improved nuclear morphology	(Varela *et al.*, 2008)
			in vivo in *Zmpste24*$^{-/-}$ mice	lifespan extension, reduced growth retardation and weight loss, reduced hair loss, improved bone density/bone mineralization/cortical thickness/kyphosis, increased adipose tissue	(Varela *et al.*, 2008)
FTIs*	prelamin A processing	prelamin A farnesylation	*in vitro* in patient or mouse cells	improved nuclear morphology	(Capell *et al.*, 2005) (Glynn and Glover, 2005) (Toth *et al.*, 2005) (Yang *et al.*, 2005)
			in vivo in *Zmpste24*$^{-/-}$ mice	lifespan extension, improved grip strength and bodyweight, reduced rib fractures, increased pQCT	(Fong *et al.*, 2006)
			in vivo in HGPS mice	lifespan extension, improved bone mineralization/cortical thickness/kyphosis/rib factures, increased adipose tissue/bodyweight	(Yang *et al.*, 2006) (Yang *et al.*, 2008)
			in vivo in HGPS mice	delayed onset of cardiovascular phenotype and delayed disease progression	(Capell *et al.*, 2008)
ICMT inhibitor	prelamin A processing	ICMT	*in vivo* in *Zmpste24*$^{-/-}$ mice	lifespan extension, increased bodyweight, normalized grip strength, reduced bone fractures	(Ibrahim *et al.*, 2013)
JH4	progerin-lamin A/C binding	progerin-lamin A/C binding	*in vivo* in HGPS mice	lifespan extension, improved nuclear morphology, increased tissue cell density, reduced senescence markers, restored gene expression, increased bodyweight, increased grip strength, suppressed hair loss	(Lee *et al.*, 2016)
NAC	oxidative stress	ROS	*in vitro* in patient cells	increased proliferation, reduced levels of DNA damage	(Richards *et al.*, 2011)
caNRF2	NRF2 re-activation	NRF2	*in vitro* in patient cells	reduced progerin accumulation, improved gene expression and levels of nuclear architectural proteins, reduced ROS and DNA damage levels	(Kubben *et al.*, 2016)
Methylene blue	mitochondrial biogenesis	mitochondria function	*in vitro* in patient cells	restored mitochondrial defects, increased proliferation, improved nuclear morphology, nuclear membrane progerin release, rescued heterochromatin loss, corrected gene expression	(Xiong *et al.*, 2016)
Morpholinos	access of splicing machinery	abnormal *Lmna* splicing	*in vivo* in HGPS mice	lifespan extension, reduced progerin transcription and accumulation, restored nuclear morphology, reduced senescence markers, improved bodyweights, reduced degree of kyphosis, normalized blood glucose	(Osorio *et al.*, 2011)
Rapamycin and analogues*	autophagy	progerin turnover	*in vitro* in patient cells	progerin clearance, increased cellular lifespan, restored nuclear morphology	(Cao *et al.*, 2011b)
			in vitro in patient cells	progerin clearance, increased proliferation, restored nuclear morphology, reduced levels of DNA damage	(Gabriel *et al.*, 2016)
Remodelin	microtubule	NAT10	*in vitro* in patient cells	improved nuclear morphology and chromatin organization, reduced DNA damage, increased proliferation	(Larrieu *et al.*, 2014)
Resveratrol	SIRT1 activity	SIRT1	*in vivo* in *Zmpste24*$^{-/-}$ mice	lifespan extension, rescued adult stem cell decline, slowed bodyweight loss, improved trabecular bone structure and mineral density	(Liu *et al.*, 2012)
			in vivo in HGPS mice	normalized external dental phenotype, reduction in ribcage fractures	(Strandgren *et al.*, 2015)
Sulforaphane	autophagy	progerin turnover	*in vitro* in patient cells	progerin clearance, increased proliferation, restored nuclear morphology, reduced levels of DNA damage	(Gabriel *et al.*, 2015)
Stem cell transplantation	stem cell function	tissue regeneration	*in vivo* in progeroid mouse model	lifespan extension, health span extension (delayed phenotype onset)	(Lavasani *et al.*, 2012)

*Drugs used in clinical trials in patients with HGPS

HGPS cells, including a reduction in misshapen nuclei and reduced progerin levels, increased proliferation, and partially ameliorated DNA damage (Gabriel *et al.*, 2016). Treatment with sulforaphane (the antioxidant derived from cruciferous vegetables) resulted in enhanced autophagy-mediated clearance of progerin, restoration of nuclear morphology, increased proliferation and reduced levels of DNA damage in HGPS patient cells (Gabriel *et al.*, 2015). In another resent *in vitro* study, it was also shown that HGPS patient cells display mitochondrial morphological and behavior defects, and that treatment with the mitochondrial-targeting antioxidant methylene blue significantly reduced the mitochondrial defects and rescued the HGPS nuclei phenotype (Xiong *et al.*, 2016). Taken together, these studies suggest promising therapeutic approaches for treatment of children with HGPS, and a clinical trial using a combination of FTI and the drug everolimus (a rapamycin analog) was initiated in April 2016 (Progeria Research Foundation, 2016).

One treatment method that has yielded conflicting results is the usage of resveratrol, a plant-produced antioxidant. In a resent study, resveratrol treatment of zmpste24-deficient mice showed rescued adult stem cell decline, increased lifespan, slowed bodyweight loss and improved bone properties (Liu *et al.*, 2012). In contrast, resveratrol treatment of a mouse model with bone-specific expression of the HGPS mutation showed no beneficial effects other than normalization of the external dental phenotype and a reduction in ribcage fractures (Paper I).

Innately elevated levels of ROS (reactive oxygen species) has been shown to cause accumulation of un-repairable DNA damage in HGPS patient cells, and treatment with the ROS scavenger NAC (N-acetyl cysteine) reduced DNA damage levels as well as increased cell proliferation (Richards *et al.*, 2011). Recent *in vitro* data suggest that progerin accumulates in the lamina and sequesters the NRF2 pathway, and that reactivation of the NRF2 pathway using constitutively activated NRF2 (caNRF2) reduced progerin levels and rescued several nuclear defects in HGPS patient cells (Kubben *et al.*, 2016).

A promising newly developed treatment strategy is gene-therapy with antisense-morpholinos, targeting the pathogenic splice site and preventing production of the truncated HGPS prelamin A protein. Treatment with these antisense-morpholinos in $Lmna^{G609G/G609G}$ mice ameliorated the HGPS phenotype and significantly extended the lifespan (Osorio *et al.*, 2011). In a study using the same mouse model, the usage of a newly identified compound, JH4, which blocks the progerin-lamin A/C interaction, showed marked improvements of several HGPS phenotypes, and in addition extended the lifespan (Lee *et al.*, 2016). As a control, they tried the same compound in zmpste24-deficient mice but saw now changes in the phenotype, indicating the progerin specificity of the compound (Lee *et al.*, 2016). Another study utilizing compound screening discovered Remodelin, a small molecule targeting the SUN1 associated acetyl-transferase protein NAT10, and subsequently restored several progeroid phenotypes in HGPS cells (Larrieu *et al.*, 2014). (Table 3)

2 AIMS OF THE THESIS

The overall aim of this thesis was to acquire a deeper understanding of the molecular mechanisms of HGPS, with a primary focus on bone tissue, and to analyze different strategies for possible treatment of HGPS.

The specific aims were:

Paper I

- To analyze the possibility of reversing a fully developed HGPS bone phenotype by silencing the mutation.
- To assess resveratrol as a treatment option for HGPS bone disease.

Paper II

- To test if long-term progerin expression in neurons resulted in tissue-pathology in the brain, in an attempt to clarify why children suffering from progeria do not develop signs of neurodegeneration.

Paper III

- To characterize the mandibular molars of a mouse model with osteoblast-, osteocyte-, and odontoblast specific expression of the most common HGPS mutation, in order to gain deeper knowledge of how the teeth are affected in HGPS.

Paper IV

- To analyze the skeletal phenotype of a previously developed mouse model with systemic expression of the progeria mutation, where a detailed assessment of the bone phenotype was lacking.
- To assess the bone marrow phenotype and possible impairment of the bone marrow derived MSC population, and its potential contribution to the development of the progeria phenotype.

3 METHODOLOGY

3.1 LABORATORY ANIMALS

3.1.1 Animal housing

Experimental mice were housed in individually ventilated cages in a 12-hour light/dark cycle at 19-23°C and 50-65% air humidity at a pathogen-free animal facility at Karolinska Institutet, Huddinge, Sweden. The mice were fed irradiated and autoclaved RM3(P) mouse pellets (SDS Diets, Essex, UK) and drinking water *ad libitum*. From postnatal week 3, softened mouse pellets were additionally provided on the cage floor (Paper I, III and IV). The Stockholm South Ethical review board and the Linköping Ethical review board approved all animal studies.

3.1.2 Generation of transgenic mice

To be able to study the effect of tissue specific expression of the most common HGPS mutation in Papers I-III, we used mice carrying the minigene of human lamin A under the control of a tet-operator (tetop-LA^{G608G}, line VF1-07). The tetop-LA^{G608G} mice were generated and maintained on FVB/N background (Sagelius *et al.*, 2008a). Humanized mouse models are also highly relevant for testing treatments for human diseases in mice.

In Papers I and III we studied the effect of progerin expression in bone tissue, and in order to generate bitransgenic mice we intercrossed tetop-LA^{G608G} mice with mice carrying the bone-specific promoter Sp7-tTA. The Sp7-tTA promoter mice were maintained on C57BL6/J background. Mice positive for both transgenes (tetop-LA^{G608G+}; Sp7-tTA^{+}) corresponded to HGPS mice, and mice negative for the transgenes (tetop-LA^{G608G-}; Sp7-tTA^{-}) corresponded to wild-type (WT) mice. Mice positive for only one of the transgenes were regarded as control mice. From postnatal week 2 and until sacrifice, mouse bodyweight and tooth status were recorded weekly. Mice up to 53 weeks of age were sacrificed for tissue collection.

For Paper II, the NSE-tTA (line A) (Chen *et al.*, 1998) promoter mice were used, which were maintained on CD1 background. To generate bitransgenic mice, NSE-tTA mice were intercrossed with tetop-LA^{G608G} mice. HGPS mice corresponded to tetop-LA^{G608G+}; NSE-tTA^{+} mice, and WT mice corresponded to tetop-LA^{G608G-}; NSE-tTA^{-}. Single transgenic mice (tetop-LA^{G608G+}; NSE-tTA^{-}) were also used in this study as control mice. Mice up to 90 weeks of age were sacrificed for tissue collection.

In the study for Paper IV, the *Lmna*$^{G609G/+}$ mouse model was used, which was kindly provided by Dr. Carlos López-Otín (Universidad de Oviedo, Spain) (Osorio *et al.*, 2011). These knock-in mice express lamin A and progerin in all tissues where lamin A is normally expressed and is regarded as the ultimate model for HGPS. The *Lmna*$^{G609G/+}$ mouse strain was maintained on C57BL6/J background. Generation of *Lmna*$^{G609G/G609G}$ mice was

accomplished by intercrossing *Lmna*$^{G609G/+}$ mice. Mice negative for the G609G transgene (*Lmna*$^{+/+}$) corresponded to WT mice. From postnatal week 2 and until sacrifice, mouse bodyweight and tooth status were recorded weekly for *Lmna*$^{G609G/G609G}$ and WT littermates.

3.1.3 PCR genotyping

DNA for genotyping was extracted from tail biopsies using either a standard phenol:chloroform isolation method with isopropanol precipitation, or the Gentra Puregene Tissue Kit (Qiagen). Presence or absence of each transgene was confirmed by PCR using primers for respective transgene, and in addition primers for *myc* were used as a positive control to ensure a good amount and quality of the isolated DNA.

3.1.4 Doxycycline administration

For Paper I, the HGPS mutation was silenced in two different groups of mice by supplementing the drinking water with 100 μg/ml doxycycline (Sigma-Aldrich) and 2.5% sucrose, beginning in postnatal week 3 and 5 respectively. Both groups of mice contained WT and tetop-LA^{G608G+}; Sp7-tTA^{+} mice. The doxycycline drinking bottles were covered in aluminum foil and changed 2 and 3 times per week. After transgenic suppression for 7, 12, 30 and 48 weeks, respectively, the mice were sacrificed.

To elucidate how fast the transgenic expression would be completely silenced in the bone tissue, a doxycycline responsiveness study was performed (Paper I). The drinking water bottles in selected breeding cages were therefore supplemented with 100 μg/ml doxycycline and 2.5% sucrose when a litter was born. The newborn pups were then sacrificed either at postnatal day 0 (PD0, before doxycycline introduction), postnatal day 3 (PD3), or at postnatal day 6 (PD6).

3.1.5 Resveratrol treatment

For the resveratrol treatment study in Paper I, the mice drinking water was supplemented with 20 μg/ml resveratrol (R5010, Sigma-Aldrich) and 2.5% sucrose from postnatal week 3 and until sacrifice at 10 weeks of age. The resveratrol was > 99% pure, as determined by GC by the manufacturer. A control group of untreated HGPS and WT mice received water supplemented with only 2.5% sucrose. The resveratrol drinking bottles were covered in aluminum foil and changed 2 and 3 times per week.

3.2 ANIMAL TISSUE COLLECTION AND PROCESSING

Animals used for tissue collection in Papers I, III and IV were sacrificed by an isoflurane (Baxter, Kista, Sweden) overdose or decapitation under isoflurane anaesthesia. In Paper II, animals were either sacrificed by cervical dislocation without anesthesia (mice used for RNA and protein extractions), or by transcardial perfusion with PBS/paraformaldehyde (PFA)

under katamine/xylazine anesthesia (mice used for histological staining, immunofluorescence and immunohistochemistry).

Tissues collected for RNA and protein extractions were dissected as fast as possible, immediately snap frozen in liquid nitrogen and stored at -80°C. Bones (femur and tibia) to be used for RNA or protein analysis were flushed clean from bone marrow by cutting the bone ends off and thoroughly flush the diaphysis with PBS using a 27-gauge needle.

For the analysis of bone marrow MSC population in Paper IV, fine dissected femurs and tibias were immediately collected to ice cold 10% FBS/PBS (Gibco) for isolation of bone marrow cells and subsequent fluorescence-activated cell sorting (FACS) phenotyping or further selection of MSCs.

Tissues to be used for histological, immunofluorescent, or immunohistochemical staining were fine dissected and fixed in 4% PFA in PBS (pH 7.4) at 4°C overnight. After the overnight incubation, the fixed tissues were transferred to 70% ethanol and stored at 4°C. All tissues except bone could be directly sent for dehydration processing and paraffin embedding without any prior processing, whereas bone tissues (femur, lower jaw, tail, and hind legs from young pups) first were decalcified in 12.5% EDTA (pH 7.0) in 4°C. Hind legs from pups collected at PD0, PD3 and PD6 were decalcified for three days, and femurs, lower jaws and tails from mice aged 3 weeks and up were decalcified for three weeks. For long-term decalcification, the EDTA was changed every 3-5 days. After dehydration and paraffin embedding, all analyzed tissues were sectioned in 4μm using a microtome. The sections were collected on Superfrost glass slides (Thermo Scientific) for histological staining, and on Superfrost Plus or Superfrost Plus Gold glass slides (Thermo Scientific) for immunofluorescent and immunohistochemical staining. All sections were dried for 1 hour at 60°C for adhesion of the sections onto the glass slides.

3.3 BONE MEASUREMENTS

The length and width of femurs and tibias from HGPS and WT mice were measured using an electronic digital caliper in Papers I and II. The total bone length was defined as the distance between the most distal part and the most proximal part of the bone. The femur length was consequently measured between the condyle and the greater trochanter, and tibia length was measured between the malleolus and the tibial tuberosity. The thickness of the bone was measured at the middle of the bone, where the thickness was defined as the distance from the anterior to the posterior side of the bone.

3.4 RNA EXTRACTION AND CDNA SYNTHESIS

3.4.1 RNA extraction

Total RNA was extracted from snap-frozen tissues (skeletal muscle, tailbone, and tibia cleaned of bone marrow) according to standard TRIzol reagent procedures according to the manufacturer's protocol (Invitrogen). Tissue homogenization was performed in ice-cold TRIzol using Lysing Matrix D tubes and a FastPrep220A instrument (Qbiogene). After resuspension of RNA in 20 µl of nuclease-free water (Gibco), the samples were diluted in 1X TE-buffer (pH 8.0) and quantified using a spectrophotometer (BioPhotometer, Eppendorf). RNA from skeletal muscle was further purified by treatment with DNase I (RQ1 RNase-Free DNase, Promega) and RNA cleanup (RNeasy Mini columns, Qiagen) according to the manufacturer's recommendations. RNA samples were stored at -80°C until use.

3.4.2 cDNA synthesis

One microgram of total RNA was reverse transcribed with random hexamers using the SuperScript® First-Strand Synthesis kit (Invitrogen). The cDNA samples were stored at -20°C.

In Paper I, transgenic expression of human lamin A and progerin on RNA level was analyzed in tailbone and tibia from HGPS and WT mice treated with doxycycline. The doxycycline treated mice were compared to untreated mice to confirm transgenic silencing. The cDNA was amplified by PCR using HotStarTaq® *Plus* DNA Polymerase kit (Qiagen) using our published RT-PCR assays for β-actin (Schmidt *et al.*, 2012), human lamin A and progerin (Sagelius *et al.*, 2008a).

3.5 DROPLET DIGITAL PCR

Droplet digital PCR (ddPCR) is based on droplet technology using water-oil emulsion. Every sample is fractionated into 15 000-20 000 droplets prior to PCR amplification, and PCR amplification of template molecules occurs in each droplet individually. In Paper I, quantitative gene expression analysis was performed using the QX200 ddPCR system (Bio-Rad). The PCR reactions were performed in 20-µl reactions using QX200 ddPCR EvaGreen Supermix (Bio-Rad) and Eppendorf® twin-tec semi-skirted 96-well plates, according to the manufacturer's recommendations. For each assay, optimal annealing temperature and cDNA template dilution were individually established. Determination of detection range for each assay was performed using serial dilutions of a cDNA control sample. All used assays had an R^2 correlation coefficient > 0.99. The sample data was only accepted when falling within the established detection ranges, and the aim was of having > 100 detected copies for each 20-µl reaction. Sirt1 expression levels were assessed in cDNA from skeletal muscle, and progerin and human lamin A expression levels were analyzed in cDNA from tibia. Analyses of β-actin expression levels were performed in all assessed samples as a control.

3.6 WESTERN BLOT

Transgenic expression at protein level was assessed using Western blot. The protein was extracted from snap-frozen tissues using 5% RIPA buffer containing 8M Urea and proteinase inhibitors (Roche). The samples were homogenized using Lysing Matrix D tubes and a FastPrep220A instrument (Qbiogene). Protein separation using Western blot was performed according to established protocols (Sagelius *et al.*, 2008a).

In Paper I, femur protein from doxycycline treated HGPS mice were compared against untreated mice, therefore a mouse monoclonal anti-human lamin A+C (mab3211, Chemicon Europe Ltd) primary antibody that do not cross-react with mouse laminA/C protein was used to analyze only transgenic expression. A mouse monoclonal anti-β-actin (A5441, Sigma-Aldrich) primary antibody was used as a control.

In Paper II, the normal protein expression levels of mouse lamin A and C were analyzed in brain, liver, kidney and bone from WT mice, using the anti-lamin A/C (N18, sc-6215, Santa Cruz Biotechnology) primary antibody. The mouse monoclonal anti-β-actin (A5441, Sigma-Aldrich) primary antibody was used as a control. Relative quantification of mouse lamin A to lamin C proteins was performed by densitometry using a VersaDoc™ Imaging System and analyzed using the Quantity One software (Bio-Rad).

3.7 STAININGS FOR HISTOPATHOLOGY

Femur, tailbone, hind leg and lower jaw sections collected on Superfrost glass slides (Thermo Scientific) were processed for Hematoxylin and Eosin (H&E) staining using an automated standard protocol. Staining with Alcian Blue (pH 2.5)/van Gieson was performed on femur and tailbone sections collected on Superfrost Plus glass slides (Thermo Scientific). For Paper I, femur osteoclasts were visualized using a tartrate-resistant acid phosphatase (TRAP) detection kit (Kit 387A, Sigma-Aldrich) according to the manufacturer's instructions. The purple TRAP staining intensity was blindly graded by two different persons, who scored the intensity from 1 (low intensity) to 4 (high intensity).

3.8 QUANTIFICATION OF EMPTY OSTEOCYTE LACUNAE

The frequency of empty osteocyte lacunae was quantified in H&E femur sections from HGPS and WT mice aged 3 weeks and up (Papers I, II and IV). All osteocyte lacunae in the diaphyseal cortical bone region were counted in each mouse and classified as previously described, where the lacunae were classified as containing live well-defined cells or being empty, containing no nuclei or a degenerated cell (Schmidt *et al.*, 2012).

3.9 IMMUNOFLUORESCENCE

Sections collected on Superfrost Plus and Superfrost Plus Gold glass slides (Thermo Scientific) were processed for immunofluorescent staining. In Paper I, femur sections were analyzed for the presence of BrdU. In Paper II, brain sections from aged HGPS and WT mice were stained for simultaneous analysis of BrdU and DCX. For Paper I, the femur sections underwent a single antigen retrieval step using 2M HCl for 30 min at 37°C. In Paper II, the brain sections underwent double antigen retrieval steps, which included microwave incubation (700W for 8 minutes in 10mM citrate buffer, pH 8.0) that was followed by a 30 minutes incubation in 2M HCl at 37°C.

Succeeding antigen retrieval, the sections were blocked using 3% normal goat serum followed by mouse-to-mouse blocking reagent (Scytek). Both blocking steps were performed for 30 minutes in room temperature. The primary antibodies used for the brain sections were anti-BrdU (1:25, 347580, BD Bioscience) and anti-DCX (1:75, ab18723, Abcam), and for femur sections only anti-BrdU (1:100, 347580, BD Bioscience) was used. Primary antibody incubation was performed overnight at 4°C. The corresponding secondary antibodies were Alexa 555-conjugated goat anti-mouse (1:100, A-2122, Life Technologies) and Alexa 488-conjugated goat anti-rabbit (1:100, A-11034, Life Technologies), which were incubated for 30 minutes at room temperature in the dark. The sections were counter-stained with DRAQ5 (1:1000, 62251, Thermo Scientific) for 5 minutes in the dark prior to mounting (ProLong® Gold Antifade Reagent, P36930, Invitrogen). Imaging was performed on a Nikon A1R, and an A1+ imaging system (Nikon corporation, Japan).

3.10 IMMUNOHISTOCHEMISTRY

Sections collected on Superfrost Plus and Superfrost Plus Gold glass slides (Thermo Scientific) were processed for immunohistochemical staining. In Paper I, femurs in hind leg sections from PD0, PD3 and PD6 pups as well as femurs from 3 weeks old mice were analyzed for the presence of transgenic lamin A/progerin expression. In Paper II, GFAP staining was analyzed in brain sections. Antigen retrieval for the staining of GFAP in brain sections was performed by incubation in 10mM citrate buffer (pH 6.0) at a 95°C water bath for 30 minutes, whereas antigen retrieval for staining lamin A/progerin in femurs required a temperature of 97.5°C.

Following antigen retrieval, the sections were blocked with 3% normal goat serum prior to anti-GFAP (1:25 000, MAB360, Millipore) or anti-human lamin A+C (1:3000, mab3211, Chemicon Europe Ltd) primary antibody incubations at 4°C overnight. The following day, biotinylated goat anti-mouse secondary antibody (1:300 for brain and 1:400 for femur, 62-6540, Zymed) was applied for 30 minutes at room temperature, followed by the label antibody (ABC Elite, Vector Laboratories) for 30 minutes at room temperature. DAB chromagen (Dako Cytomation) was applied for 3 min on brain sections and 2 minutes on femur sections, followed by rinsing with distilled water. The sections were counter-stained

with Mayers haemotoxylin (1:10, Histolab), and then mounted with Pertex mounting medium for light microscopy (Histolab).

3.10.1 Quantification of immunohistochemical staining in bone

Quantification of cells expressing transgenic lamin A/progerin was conducted in the femur diaphyseal cortical bone region using a Nikon Eclipse E1000 microscope (Papers I and II). In Paper I, the frequency of transgene-positive osteocytes was quantified in the whole diaphyseal cortical bone region. In Paper II, a minimum of 2000 osteocytes were counted for each animal, and then the number of transgene-positive osteocytes in the same region were counted to calculate the frequency of osteocytes expressing transgenic lamin A/progerin.

3.11 BRDU LABELING

To monitor cell division *in vivo*, labeling with 5-Bromo-2 -deoxyuridine (BrdU) is used in cell proliferation analysis as it incorporates into newly synthesized DNA during cell division and therefore marks proliferating cells.

In Paper I, BrdU labeling was used to assess possible differences in femur growth plate chondrocyte proliferation in resveratrol- and sucrose-treated HGPS and WT mice. The mice were injected intraperitoneally with 250 mg/kg bodyweight BrdU (Sigma-Aldrich) 16 hours prior to sacrifice. Counting a minimum of 300 chondrocytes in the femoral growth plates performed the frequency quantification of BrdU-positive chondrocytes. The numbers of BrdU-positive chondrocytes were normalized against the total number of cells counted prior to comparisons between the different sample groups.

In Paper II, BrdU labeling of dividing hippocampal cells was used to monitor neurogenesis in adult HGPS and WT mice, where the aim was to determine if long-term expression of progerin had an effect on adult neurogenesis. The mice were injected intraperitoneally with 50 mg/kg bodyweight BrdU (Sigma-Aldrich) for every 24 hours during 5 consecutive days. The mice were subsequently sacrificed 16 days after the first day of injection. The whole hippocampus was sectioned and every 10^{th} section was stained for BrdU/DCX (a marker for immature neurons) where positive neuronal cells were counted. A total of 8 sections were analyzed per mouse.

3.12 BONE MARROW EXTRACTION AND MSC ISOLATION

For Paper I, bone marrow mononuclear cells were extracted from HGPS and WT mouse bones as previously described (Mansour *et al.*, 2012). Briefly, femurs and tibias were fine dissected, cut into small pieces and vigorously pipetted in PBS. The bone pieces were removed by filtering through a 40μm cell strainer. After incubation with the antibodies APC-Lineage cocktail (#558074), PE-SCA1 (D7, #562059), PerCP-Cy5.5-cKit (2B8, #560557)

and FITC-CD45 (30F11, #561088) for 15 minutes at 4°C in the dark, the bone marrow cells were washed, filtered through a 35µm cap cell strainer (352235, Falcon®) and sorted using a FACS Aria (BD Biosciences). All antibodies were purchased from BD Biosciences.

For Paper IV, femurs and tibias from WT, *Lmna*^{G609G} homozygous and heterozygous mice were fine dissected and crushed in 10% FBS/PBS (Gibco) and processed as previously described to isolate mononuclear cells (Figure 7) (Qian *et al.*, 2013). Mononuclear bone marrow cells were stained using the antibodies PE-CD51 (#104106), PE-Cy5-TER119 (#116210), PE-Cy7-CD31 (#102418), APC-Cy7-CD44 (#103028), PB-SCA1 (#108120) (all from BioLegend), and PE-Cy5-CD45 (#15-0451-81) and PE-Cy5-CD19 (#15-0193-81) (both from eBioscience) for 15 minutes at 4°C. The cells were resuspended in propidium iodine (PI, 1:1000) solution and filtered through a 35µm cap cell strainer (352235, Falcon®) prior to FACS analysis using a BD LSRFortessa II (BD Biosciences).

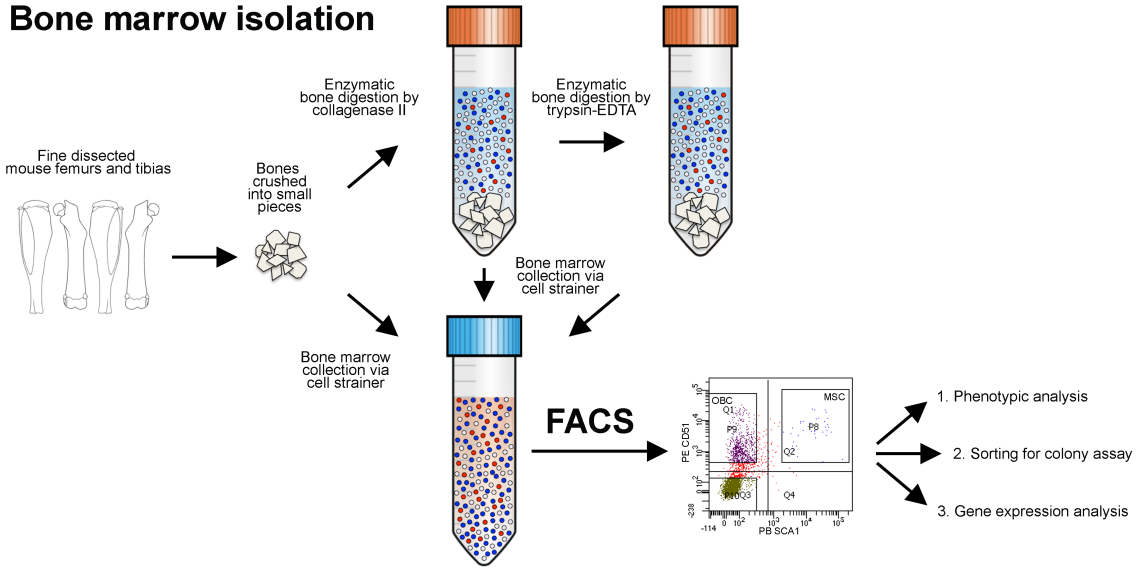

Figure 7. Experimental workflow from bone marrow isolation to analysis of MSCs. Mouse femurs and tibias were fine dissected and crushed. Bone marrow from the crushed bones was collected via a cell strainer. Subsequent enzymatic digestion and cell collection from the crushed bones was performed. Collected bone marrow cells were subjected to FACS and used in three different analysis steps: (1) Phenotypic analysis; (2) Sorting for colony assay; and (3) Gene expression analysis. Figure from Paper IV.

3.13 FLUORESCENCE-ACTIVATED CELL SORTING

In Paper I, isolated bone marrow cells were sorted using a FACS Aria (BD Biosciences). Hematopoietic stem cells (HSCs) were selected by gating for Lin^{neg}/SCA1^{pos}/cKit^{pos} cells, and MSCs were defined as Lin^{neg}/CD45^{neg}/SCA1^{pos} cells. The femur and tibia bone marrow cells were isolated and sorted separately to elucidate any possible differences between the different bones. The cell counts were normalized against the total number of analyzed cells prior to comparisons.

In Paper IV, the isolated bone marrow cells were run on a BD LSRFortessa II (BD) instrument for phenotypic characterization of the MSC and osteoblast progenitor cell (OBC) fractions. Dead cells were excluded by PI staining, where live cells were negative for PI. MSCs were defined as $CD45^{neg}/TER119^{neg}/CD19^{neg}/CD31^{neg}/CD44^{neg}/CD51^{pos}/SCA1^{pos}$ and OBCs were defined as $CD45^{neg}/TER119^{neg}/CD19^{neg}/CD31^{neg}/CD44^{neg}/CD51^{pos}/SCA1^{neg}$. MSC and OBC counts were normalized against the total number of counted cells prior to comparisons.

4 RESULTS AND DISCUSSION

4.1 PAPER I

Transgene silencing of the Hutchinson-Gilford progeria syndrome mutation results in a reversible bone phenotype, whereas resveratrol treatment does not show overall beneficial effects

The possibility of treating an extremely rare genetic disorder like HGPS, which only affects approximately 1 in 20 million individuals (Gordon, 2016), is dependent not only on the drugs used, but also on the actual ability of the affected tissues to recover. Our lab has previously showed that the HGPS skin phenotype is reversible in mice (Sagelius *et al.*, 2008b) if the transgene is turned off before a certain time point. In this study, we wanted to investigate the possibilities of reversing the HGPS bone phenotype, and to assess the potential benefits from treatment of HGPS mice with resveratrol.

To perform this study, we used a previously published mouse model with osteoblast- and osteocyte-specific inducible transgenic expression of the most common HGPS mutation in exon 11 of the *LMNA* gene (c.1824C>T, p.G608G) (Schmidt *et al.*, 2012). These mice develop a bone phenotype that closely resembles the bone abnormalities seen in HGPS patients, including growth retardation, abnormal gait, empty osteocyte lacunae, adipocyte infiltrated bone marrow, bone mineralization defects and compromised bone quality and strength, and dental defects. Since this mouse model is based on the Tet-Off system, supplementation of doxycycline would suppress the transgenic expression of the HGPS mutation. Since HGPS is a very rare disease, discovering that a child is suffering from progeria will not happen until the clinical symptoms are already present. For this reason, in this study we waited until the mice had already developed a visible phenotype before initiating silencing of the transgenic expression or treatment with resveratrol. To mask any possible bad taste of doxycycline or resveratrol, drinking water containing these compounds was also supplemented with sucrose. This study consisted of different treatment groups (doxycycline, resveratrol and sucrose alone) and animals were analyzed at several time points: after treatment for 7, 12, 30 and 48 weeks, respectively (Figure 8). Silencing of transgenic expression by adding doxycycline to the mouse drinking water began at postnatal week 3 or 5, whereas resveratrol and sucrose treatments were initiated solely at postnatal week 3, since that was the earliest time point for a visible appearance of the progeria bone phenotype in this mouse model. Transgenic suppression from two different time points gave us the opportunity to study whether the timing would be crucial when removing progerin expression. We chose to begin suppressing the transgene at the beginning and at the end of the mouse growth spurt. Two resulting scenarios were plausible: (i) the earlier the progerin production would be halted, the better the chances would be for a full recovery; or (ii) since bone is a continuously remodeling tissue, timing should not significantly matter.

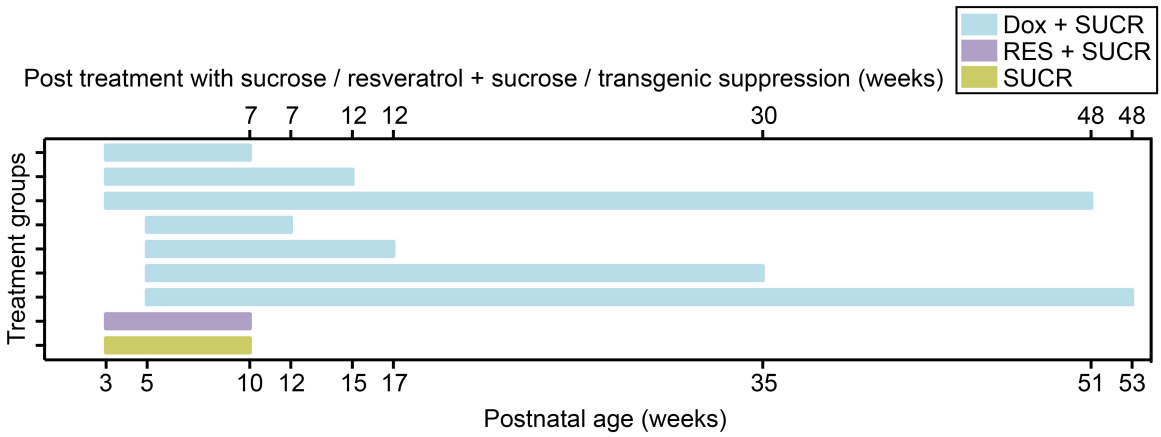

Figure 8. Experimental outline. HGPS and WT mice were treated with doxycycline and sucrose (Dox + SUCR), resveratrol and sucrose (RES + SUCR), or sucrose alone (SUCR) for different periods of time. Treatments began at either postnatal week 3 or 5.

A crucial result in this study was that we could show that the transgenic expression in our system was tightly regulated by doxycycline, and in addition that complete transgenic suppression was attained within 6 days of treatment, although the majority of transgene-expressing cells had been silenced within 3 days. These findings were demonstrated by RT-PCR and Western blot on bone tissue, as well as by immunohistochemical staining of hind legs.

Silencing the transgenic expression from either postnatal week 3 or 5 generally resulted in very different degree of improvement in the mice. While mice silenced from postnatal week 3 showed substantially improved bodyweight gain, complete elimination of ribcage calluses, and significantly fewer femoral empty osteocyte lacunae with each time point analyzed (initial 84% before silencing and 10% after silencing for 48 weeks), the mice silenced from postnatal week 5 did not show any improvement in rate of weight gain compared to sucrose-treated mice, and they still displayed ribcage calluses even after silencing for 48 weeks (Table 4). However, the mice silenced from postnatal week 5 did show a significantly reduced frequency of empty osteocyte lacunae (31% after silencing for 48 weeks), though not as striking as the improvement displayed by the mice silenced from postnatal week 3. In conclusion, the results from this part of the study indicate that the earlier the HGPS mutation could be silenced, the better the chances are for recovery. Since the human skeleton is remodeled approximately every decade, our results may therefore indicate that if the HGPS mutation could be silenced in progeria patients, skeletal improvements could be substantial.

Treating the HGPS mice with resveratrol generally resulted in the same improvements as treatment with sucrose alone (Table 4). However, the reversal of the external dental phenotype of overgrown and laterally displaced lower incisors in HGPS mice could be attributed to resveratrol. In addition, the presence of ribcage calluses was significantly reduced in the resveratrol-treated mice compared to sucrose-treated mice, which could

indicate either a protective effect against fractures or improved fracture-healing abilities when resveratrol is ingested. As compared to another study, where resveratrol-treatment of zmpste24-deficient mice yielded beneficial effects such as slowed bodyweight loss and improvements in the bone tissue (Liu *et al.*, 2012), the beneficial effects from resveratrol-treatment in our study were rather modest. A reason for these differences is the use of two completely different mouse models: zmpste24-deficient mice have a systemic lack of *Zmpste24* and accumulate prelamin A, whereas our mouse model produces both normal mouse lamin A and human lamin A and progerin in a restricted tissue. In our study, we initiated resveratrol-treatment first after development of a phenotype, whereas Liu *et al* (2012) introduced resveratrol to newborn mice and in addition had twice as long treatment duration as in our study. Combining these aspects, it is not unlikely that the results from the two different studies would be different.

In summary, this study shows that the HGPS bone defects to a large extent indeed are reversible if the mutation can be suppressed or abolished, which in turn gives hope for the future development of treatments for progeria.

Table 4. Bone and dental phenotypes in HGPS mice, and following transgenic suppression, treatment with resveratrol + sucrose and treatment with only sucrose.[1]

Phenotypes (previously characterized by (Schmidt *et al.*, 2012))	**HGPS mice from postnatal week 3 and onwards**	**Duration of transgenic suppression by treatment with doxycycline + sucrose (weeks)**		**Duration of resveratrol + sucrose treatment (weeks)**	**Duration of sucrose treatment (weeks)**
		7[a]	**12-48[a]**	**7**	**7**
Bone					
Shortened bone length	✓	✓[b]	NA	✓[b]	✓[b]
Ribcage callus	✓	✓[b]	Recovered[c]	✓	✓
Irregular and deformed femur cortex lacking lamellar structure	✓	Partially recovered	Partially recovered	✓	✓
Empty osteocyte lacunae	✓	Partially recovered	Partially recovered	✓	✓
Hypocellular bone marrow	✓	Recovered	Recovered	Recovered	Recovered
Adipocyte infiltration in the bone marrow	✓	Recovered	Recovered	Partially recovered	Partially recovered
Non-remodeled/non-mineralized bone matrix	✓	Partially recovered	Recovered[c]	✓	✓
Reduced osteoclast activity	✓	Recovered[d]	NA	✓	NA
Dental					
Overgrown and outward bent lower incisors	✓	Recovered[c]	Recovered[c]	Partially recovered	✓
Disorganized incisor odontoblasts layer	✓	Recovered	Recovered	✓	NA
Incisor dentin demarcation line	✓	Recovered	Recovered	✓	NA
Disorganized molar odontoblasts layer	✓	✓	✓	✓	NA
Molar dentin demarcation line	✓	✓	✓	✓	NA

Each phenotype was assessed against age-matched wild-type littermates. [a]Transgenic suppression began at postnatal weeks 3 and 5 and the results were the same unless otherwise specified. [b]Significant improvement was noted when compared to untreated HGPS mice. [c]HGPS mice with suppressed transgenic expression from postnatal week 3, but not postnatal week 5, recovered. [d]Only mice silenced from postnatal week 3 were analyzed. ✓, phenotype present; NA, not analyzed.

(Strandgren *et al.*, 2015)[1]

4.2 PAPER II

Expression of progerin in aging mouse brains reveals structural nuclear abnormalities without detectible significant alterations in gene expression, hippocampal stem cells or behavior

Although lamin A is expressed in all terminally differentiated cells and tissues, the HGPS phenotype is segmentally restricted to certain tissues, mainly of mesenchymal origin. For example, skin and bone are strongly affected in HGPS, while one of the seemingly unaffected tissues is the brain. One suggested reason for the lack of pathological age-associated features in the brain of progeria patients, such as dementia, is due to the fact that the children do not get old enough for this type of disease to develop. In this study, we therefore sought to analyze the effects of long-term neuronal expression of the most common HGPS mutation (*LMNA* c.1824C>T, p.G608G), to test the hypothesis that neuropathological alterations would likely occur if the progeria patients were to live longer. Hence, we developed an inducible transgenic mouse model with expression of the HGPS mutation restricted to the brain, skin, bone and heart by utilizing the NSE-tTA promoter mice (Chen *et al.*, 1998), in order to investigate how these organs would be affected by long-term exposure of progerin. Mice up to 90 weeks of age were analyzed for signs of pathology, both histologically and by behavioral studies.

Since accumulation of progerin has been suggested to cause the progressive nature of HGPS, we analyzed the accumulation of transgenic lamin A/progerin or progerin in the brain, bone, skin and heart from HGPS mice of different ages using immunofluorescence with specific antibodies. In the brain, as many as 91% of the cells in the hippocampus showed transgenic expression, and progerin accumulated in both the hippocampus and frontal cortex with advanced age. Analysis of heart tissues did not show any significant accumulation of transgenic progerin. In the bone tissue, aged HGPS mice showed a significantly decreased frequency of transgene-positive osteocytes compared to young HGPS (<1% and 8.1%, respectively). These numbers could be compared to our previously published mouse model with bone-specific expression of the most common HGPS mutation, where the great majority of the osteocytes were transgene-expressing (92%) when using the Sp7 transactivator (Paper I). Since we had also previously showed a significant reduction in the number of osteocytes in mice expression the HGPS mutation specifically in bone, the frequency of empty osteocyte lacunae was quantified in order to rule out that increased loss of osteocytes caused the lower number of transgene-expressing cells in the older mice. However, there was no evidence suggestive of loss of osteocytes. To determine if the progerin expression and accumulation had an effect on adult cell proliferation and neurogenesis in the brain, the hippocampal region of aged mice were analyzed. Quantifications showed however no difference in frequency of proliferating cells or neurogenesis. Taken together, these results indicated a higher transgenic expression and progerin accumulation in the HGPS brain compared to WT mice and the other analyzed tissues in this mouse model, but no subsequent effect on adult neurogenesis.

The only externally visible phenotype that could be observed for the HGPS mice was their slightly smaller size and reduced capacity to gain weight as they aged, which was confirmed by weight data as well as size measurements of the femur and tibia from different mouse ages. Data analysis showed that HGPS mice were significantly smaller than WT mice regarding both bodyweight and bone lengths. If this bone size reduction (and therefore in part probably also the total body size reduction) can be completely attributed to the relatively low frequency of transgene expressing osteoblasts and osteocytes is difficult to tell. The reason for this is mainly because the youngest age analyzed for these measurements was 20 weeks of age, an age well beyond the mouse growth spurt, which is a time period when impaired osteoblasts might cause a reduced growth. For this reason, it would have been interesting to also analyze younger mice, i.e. 3 weeks old, to elucidate if the frequency of transgene expressing bone cells were higher than the modest 8.1% seen at 20 weeks, or if maybe also the growth plate chondrocytes (responsible for lengthening the bone) expressed the transgene in an early developmental stage. In addition to the bone and weight measurements, histological analysis of the skin showed a considerable loss of subcutaneous fat in aged HGPS mice, which would in part explain the reduced capacity to gain weight with advanced aging. There were no apparent changes in behavior when comparing HGPS to WT mice, not even after analyzing the results of a carefully conducted behavioral study.

Ultrastructural analysis of the brain, white adipose tissue and bone from 70 weeks old mice revealed severe distortions, with multiple lobulations and irregular extension, in 95.5% of the hippocampal neurons of HGPS mice, compared to only 11% in the WT mice. However, there was no apparent loss of heterochromatin in HGPS mice compared to WT. In the bone, there were no apparent alterations in the nuclear structure of osteoblasts and osteocytes, whereas 46% of the HGPS adipocytes showed nuclear irregularities compared to 25% in the WT mice.

Since almost all neurons in the brain from aged HGPS mice showed severe nuclear distortions, global genome transcript analysis was performed on RNA extracted from hippocampus from aged HGPS and WT mice, in order to investigate whether any changes in gene expression were present. Unexpectedly, despite the severe distortions in the hippocampal neuronal nuclei there were only negligible changes in gene expression, where only five genes (out of the 16 572 RefSeq genes analyzed) showed a significant 2-fold change.

In summary, careful pathologic examinations of aged HGPS mice did not show any neuropathological changes or altered gene expression, despite severe neuronal nuclear distortions and transgene expression in 91% of the hippocampal cells, even after 90 weeks of progerin expression. This is indeed surprising, especially if these results are compared to the findings in our mouse model with bone-specific expression of the HGPS mutation, where the same amount of transgene expressing cells (92% of bone tissue osteocytes) caused major alterations in the bone tissue and a clear HGPS bone disease pathology (Paper I and (Schmidt *et al.*, 2012)). Our results therefore support the hypothesis that neuronal cells are less

sensitive to, or protected from, the functional deleterious effects of progerin expression, which might be explained by that differentiated neurons are post-mitotic and therefore no longer proliferating. Our results also show that severe nuclear distortions do not automatically induce changes in gene expression or functional changes in hippocampal activity.

4.3 PAPER III

Expression of the Hutchinson-Gilford Progeria mutation disturbs secondary dentin formation but promotes tertiary dentin formation

Children suffering from HGPS display abnormal and delayed dentition, and formation of irregular secondary dentin obliterating the dental pulp. The dentin is produced by odontoblasts, which are specifically differentiated cells of mesenchyme origin. Unlike other cell types derived from the same source, molar odontoblasts show unique features such as a well-shaped junctional complex, and as the molar odontoblasts become terminally differentiated cells there is no ongoing replacement with newly differentiated odontoblasts. Three different types of dentin have been identified in teeth: (i) primary dentin, which forms rapidly in association with apposition of enamel or cementum during tooth formation; (ii) secondary dentin, resulting from the slow and continued apposition of dentin in later life; and (iii) tertiary dentin (reactive or reparative), which is deposited beneath the site of injury by surviving pulp tissue odontoblasts as a local response to trauma. The tertiary dentin matrix secreted by these odontoblasts results in an increase in metabolic activities of the cells.

We have previously reported that bone tissue-specific expression of the most common HGPS mutation (c.1824C>T, p.G608G) results in formation of irregular dentin formation and polarization defects in odontoblasts (Schmidt *et al.*, 2012). In this study, we used the same inducible transgenic mouse model to further analyze how progerin expression in the bone might contribute to the mandibular molar dentin abnormalities in HGPS.

Transgenic lamin A/progerin expression could only be found in odontoblasts of 3 weeks old HGPS mice. Analysis of total dentin formation with age showed that the coronal dentin thickness of HGPS mice was significantly thinner at postnatal weeks 3 and 5 compared to WT. By week 20 however, the HGPS mice had accelerated their dentin production and deposited more dentin than WT mice, resulting in a significantly thicker dentin in HGPS mice. Histological analysis of the dentin indicated a loss of predentin in HGPS mice, but that the primary dentin layers were similar for both genotypes, although different in thickness. The HGPS secondary dentin formation was however markedly impaired, with abnormal tertiary dentin deposited beneath the primary dentin instead, separated by a clear demarcation line. In adult HGPS mice (13 and 20 weeks old), almost the entire pulp chamber and root canals were filled with excessively deposited tertiary dentin. These data indicate that early progerin expression in odontoblasts disturbed formation of secondary dentin and instead promotes formation of tertiary dentin in HGPS mice, whereas the formation of primary dentin was unaffected.

Microstructural analysis of the dentin showed that although HGPS mice had substantially thinner primary dentin compared to WT mice, no differences could be observed in the micro-structure. However, the secondary/tertiary dentin structure was utterly different between HGPS and WT mice, where instead of the normal and regular tubular structures, the HGPS dentin was irregular and porous. Immunohistochemical staining of adult mice revealed that dentin matrix protein-1, which is essential for proper dentin and bone mineralization, was extensively localized in the secondary/tertiary dentin of HGPS mice, but could rarely be found in the secondary dentin of WT, indicating that mineralization was ongoing in HGPS mice. These results add further evidence to the indication that progerin expression does not significantly affect the formation of primary dentin in HGPS, and that HGPS mice lack proper secondary dentin and instead deposit tertiary dentin.

In summary, this study showed that expression of the HGPS mutation in odontoblasts significantly disturbs secondary dentin formation in the mandibular molars, and that instead tertiary dentin is deposited, likely as a consequence of progerin expression. Since tertiary dentin is deposited as a response to injury, these results indicate that HGPS mouse molars are subjected to trauma, and as active mineralization of the tertiary dentin was present it is plausible that this trauma is continuous. In total, these findings could be used to further analyze the mechanisms involved in formation of reactive/reparative tertiary dentin, which could possibly be used in a clinical setting to stimulate tertiary dentin formation when needed.

4.4 PAPER IV

Phenotypic analysis of bone marrow from Hutchinson-Gilford progeria mice suggests a lower mesenchymal stem cell count

The majority of the tissues that are affected in HGPS are of mesenchymal origin, such as bone, adipose tissue, skin and cardiovascular muscle tissue. Previous studies from both our research group and others have shown that the adult stem cells are impaired in HGPS (Scaffidi and Misteli, 2008; Rosengardten *et al.*, 2011), and it has also been shown that progerin interferes with proliferation and differentiation of MSCs *in vitro* (Scaffidi and Misteli, 2008; Zhang *et al.*, 2011; Xiong *et al.*, 2013). In this study, we wanted to assess the possible impairment of the bone marrow derived MSC population in HGPS, and its potential contribution to the development of the progeria phenotype.

To perform this study we took advantage of the previously published $Lmna^{G609G}$ mouse model, where $Lmna^{G609G/G609G}$ mice express lamin A and progerin in tissues where lamin A is normally expressed and closely recapitulate the pathophysiology seen in HGPS patients, comprising a shortened lifespan, severe growth failure and subsequent reduction of bodyweight, bone alterations, and cardiovascular abnormalities including loss of vascular smooth muscle cells (Osorio *et al.*, 2011).

Since a detailed assessment of the bone phenotype of this mouse model was lacking, we analyzed the skeletal phenotype. We chose to analyze homozygous mice at 11 and 15 weeks of age, two time points corresponding to an age prior to onset of a severe phenotype and premature death, and an age where mice would be expected to have developed a severe phenotype and approximately 50% of the mice had prematurely died, respectively. We also decided to analyze adult (> 30 weeks old) $Lmna^{G609G/+}$ heterozygous mice since they also start developing a HGPS phenotype with premature death from approximately 7 months of age. While we could show a significantly higher frequency of empty osteocyte lacunae in cortical bone tissue from $Lmna^{G609G/+}$ mice compared to WT (8.6% and 3%, respectively), the increase was not as remarkable as the 84% empty lacunae that we have previously reported in our mouse model with bone-specific expression of the most common progeria mutation (Paper I). There were also no significant histopathology abnormalities in bone marrow cellularity or bone mineralization properties in the progeria compared to WT mice, another difference compared to the mouse model used in Paper I. Future studies will assess also homozygous mice of advanced age for all these properties, in order to elucidate if the discovered lack of these particular bone alterations simply might be caused by a too low expression of progerin and become more advanced at later time points. Analysis of the presence of ribcage callus formation on the other hand did reveal significantly more calluses in $Lmna^{G609G}$ homozygous and heterozygous mice compared to WT, indicating ongoing healing of fractures close to the costovertebral junctions, similar to the tissue-specific HGPS mouse model used in Paper I. Taken together, this suggests that the skeleton of $Lmna^{G609G/+}$ and $Lmna^{G609G/G609G}$ mice in total is less heavily affected as compared to our previously published bone-specific HGPS mouse model (Paper I and (Schmidt *et al.*, 2012)). The reasons for this difference could be the level of progerin being expressed, the different strain backgrounds or in which cells progerin is in fact being expressed.

Our careful analysis of MSC and OBC fractions showed that $Lmna^{G609G}$ mice had a significantly reduced frequency of MSCs compared to WT mice, whereas the frequency of OBCs was similar between the two genotypes. Sorting results also indicated a reduction in the MSC population, as overall fewer MSCs could be sorted from progeria mice than from WT mice. The older homozygous mice analyzed showed a more evident reduction in the frequency of MSCc compared to the younger homozygous mice. Assessment of the colony forming capacity of sorted MSCs indicated that only the cells from the older homozygous mice were impaired, resulting in fewer colonies formed compared to age-matched WT. These results together suggested an impaired MSC population in the progeria mice, and that the greater impairment might be caused by progerin accumulation. Contradicting to these results, analysis of proliferative capacity by further culture expansion, as well as analysis of adipogenic and osteogenic MSC differentiation potential, indicated hyperproliferation of homozygous MSCs compared to WT. Increased proliferation has previously been reported in mice with skin-specific expression of the HGPS mutation and in HGPS fibroblasts (Bridger and Kill, 2004; Sagelius *et al.*, 2008a). Taking these results together, the progeria MSC population appears to be impaired, whereas their differentiation capacity instead seems to be

going into overdrive. What might be causing this phenomenon is difficult to tell, but gene expression analysis of undifferentiated MSCs as well as MSCs differentiated into adipocytes and osteoblasts could possibly provide some clues. One theory could also be that increased proliferation is a kind of built-in compensatory mechanism.

In summary, our results suggest that mesenchymal stem cell transplantation might be a treatment strategy for HGPS that could be tested in this animal model. This model also presents the severe loss of vascular smooth muscle cells and adipose tissue that all progeria patients experience that could also be assessed for improvement following transplantation.

5 CONCLUSIONS

Paper I

- We have shown that an already developed HGPS bone disease phenotype to a large extent is reversible in mice with bone-specific expression of the most common HGPS mutation.
- An earlier suppression of the HGPS mutation results in a better recovery of the HGPS bone disease phenotype.
- Treatment with resveratrol resulted in very few beneficial effects.
- Since the human skeleton is remodeled approximately every decade, our results suggest that if the HGPS mutation could be suppressed in progeria patients, skeletal improvements could be substantial. This gives hope for the future treatment of children with progeria.

Paper II

- We have developed an inducible transgenic mouse model with expression of the most common HGPS mutation in brain, and to a lesser extent also in bone, skin and heart.
- Long-term expression and accumulation of progerin in the brain result in severe neuronal distortions with multiple lobulations and irregular extensions.
- Progerin-expressing mice more than one year old did not experience any neuropathological changes or altered gene expression, despite severe nuclear distortions.
- Our results suggest that neuronal cells are less sensitive to the functional deleterious effects of progerin expression.

Paper III

- We showed that expression of the most common HGPS mutation in odontoblasts significantly disturbs secondary dentin formation in the mandibular molars.
- Excessive deposition of irregular tertiary dentin is likely a consequence of progerin expression.
- Our findings could be used to elucidate the mechanisms involved in formation of reparative tertiary dentin, which might be applied in a clinical setting to stimulate tertiary dentin formation when needed.

Paper IV

- We showed a significantly higher frequency of empty osteocyte lacunae in cortical bone tissue from *Lmna*$^{G609G/+}$ knock-in mice compared to WT.

- There were more calluses in both *Lmna*^{G609G} homozygous and heterozygous mice compared to WT, which indicates that *Lmna*^{G609G} mice were more sensitive to fractures.

- The MSC population, adipogenic and osteogenic differentiation capacity is altered in this progeria mouse model.

- Mesenchymal stem cell transplantation is a treatment strategy that could be tested in HGPS.

6 FUTURE PERSPECTIVES

Even though the clinical trials performed so far in patients with HGPS have generated encouraging results, including improvements in weight gain and reduction of vascular stiffness in many of the patients, in addition to an extension in lifespan (Gordon *et al.*, 2014a), the total improvements were limited. As of April 2016, a clinical trial using a combination of FTIs and everolimus is ongoing (Progeria Research Foundation, 2016). However, there is still a need to gain a deeper understanding of the molecular mechanisms causing HGPS, and to evaluate other complementary methods of treatment.

In Paper I we could show that the skeletal phenotype of HGPS to a large extent could be reversed upon suppression of the HGPS mutation. Being able to turn off the expression of progerin is one of the great advantages of using transgenic mouse models; unfortunately that is not possible to do in the children with progeria, given that gene targeting and gene editing methods are not ready for clinical trials in patients yet. When the issue of drug delivery is resolved, and targeting the affected tissues in HGPS is possible and safely assessed in animal models, a gene therapy treatment approach will be feasible. Since cardiovascular disease is the primary cause of death in HGPS (Merideth *et al.*, 2008), the primary focus should be in finding a method to specifically target the vascular smooth muscle cells.

For now, we instead have to try to find other ways of treatment. If you for example only regard the skeletal phenotype of HGPS, one way to obtain more knowledge of the effects from progerin expression and to find potential targets for treatment, would be to select only the progerin expressing cells from different ages of our HGPS mouse model using the Sp7 transactivator and perform single-cell RNA sequencing. This would give the possibility to find alterations in gene expression compared to corresponding healthy cells from wild-type mice. In addition to analyzing the change of gene expression with time as progerin accumulates, it would also be interesting to investigate what happens when expression of the HGPS mutation is suppressed. How cells for analysis might be selected is another question to answer. Sorting by FACS for single-cell analysis is one obvious option. Another option could be to capture single cells from fixed tissue by laser capture micro-dissection, which is an automated sample preparation technique in which the cells are selected under microscopic visualization. The differences in gene expression between early and late transgene-expressing mice, or compared to transgene-suppressed mice, might show potential targets for the treatment of progeria bone disease. Single-cell RNA sequencing of cells from the $Lmna^{G609G}$ mouse model would of course provide a greater opportunity to analyze the effects of progerin expression on different cell types and find potential novel signaling pathways to target.

Since we in Paper IV could conclude that the MSC population is impaired in progeria, performing MSC transplantation in this mouse model would be of particular interest. For this kind of studies one might consider two different approaches that would both increase the understanding of HGPS. The first approach would be to transplant normal healthy MSCs into progeria mice and analyze the effect on measures such as survival, growth, and alterations in

bone, adipose tissue and cardiovascular system by histopathology, immunohistochemistry and immunofluorescence. To easier evaluate engraftment of healthy donor MSCs, donor mice would be eGFP-expressing mice, which enables tracking of the transplanted cells by green fluorescence. This would give information of the potential of MSC transplantation as a therapy for progeria. The second approach would be to do the opposite, i.e. to transplant MSCs expressing the progeria mutation into healthy mice and evaluate these mice for development of a progeroid phenotype. This approach would assess if progerin expression in MSCs alone is enough to cause premature aging, and might also give further answers to the contribution of progerin in normal tissue aging.

Recent data suggest that progerin accumulates in the lamina and sequesters the NRF2 pathway in cells (Kubben *et al.*, 2016), this needs to be further evaluated in animal model systems. In addition, drugs that have shown potential *in vitro* in cell cultures, such at Remodelin (Larrieu *et al.*, 2014), sulforaphane (Gabriel *et al.*, 2015), rapamycin and analogues (Cao *et al.*, 2011b; Gabriel *et al.*, 2016), and methylene blue (Xiong *et al.*, 2016), need to be further evaluated *in vivo* in HGPS animal models.

7 ACKNOWLEDGEMENTS

First of all, I would like to thank my supervisor **Maria Eriksson**. You are one of the most intelligent and inspiring people I know, and I will forever be grateful for the opportunity you gave me to be a part of your research group. Your mind is always so far ahead, that no matter how well prepared I have been for a meeting, you always seem to ask the questions I hadn't even begun thinking about. Thank you for your great guidance, support and always believing in me during these years.

My co-supervisor **Ola Nilsson**, thank you for your support and immediate help whenever I needed it. Thanks to **Elisabet Hollén**, you have been my mentor ever since I did my master thesis at LiU, having you as my supervisor. You showed me how fun research is, and you were the one who got me thinking about doing a Ph.D. in the first place.

Many thanks to **Karl Ekwall**, chairman of the Department of Biosciences and Nutrition, and former chairman **Karin Dahlman-Wright**, for providing this excellent and well-equipped place of research.

I would like to thank all the present and past members of the ME-group. **Gwladys Revêchon**, you started as a master student in the lab, and in the end you made the wonderful decision to stay for your Ph.D. studies. For almost a year now we have been working together in the MSC project, sometimes coming to the lab way before the trains even start running. You are an amazingly hard worker, and never with any complaints. Good luck with the second half of your Ph.D.! **Agustín Sola Carvajal**, our wonderful Spanish little guy! As the most senior postdoc in the lab, you know that you are expected to give a toast, right? Jokes aside, you are a wonderful colleague and a hard worker, and if you start your own lab in the future I might come knocking on the door. **Hafdís Helgadóttir**, the other Ph.D. student in the lab. You are always so happy, telling the funniest things about Iceland or planning what crazy hard races you are trying to get everyone in the lab to do. Best of luck to you as well in the remaining half of your Ph.D.! **Irene Franco**, I love listening to you presenting your work on our group meetings, I think that you are a very good speaker. I look forward to our lunches outside this summer; it is a great pleasure to have someone else in the lab that enjoys the sun as much as I do. And let's see if we end up in BB together in August! **Peter Vrtacnik**, what can I say? Until just recently, I didn't know that you were addicted to Stroopwafels. Never saw that one coming. You are just full of surprises, aren't you? What isn't a surprise though is that you are a great researcher, both to work with and talk to. **Pär Lundin**, you are the newest postdoc addition to the group. We haven't had the chance to work together, but it is always fun to have a fellow Swede around who gets what I'm trying to describe sometimes. Thanks to **Eva Schmidt** and **Hasina Nasser,** for introducing me to the world of bone tissue. **Tomás McKenna**, thank you for taking care of me and showing me around when I first came to the lab, and for being the easy-going person that you are. The first time I met you, you asked how I felt about camping and if I wanted to join sometime. I still haven't done it, but you have never stopped asking whenever you are organizing a trip. To **Jean-Ha Baek** and **Nikenza**

Viceconte, for sharing your excellent knowledge in research. **Raquel Pala Rodrigues**, you are such a nice, calm and intelligent person, and it was a great pleasure having you around. **Ylva Rosengardten**, when I had been in the lab for a day or two you came back from your summer vacation and asked, "What's new?". "ME!" I said. I think that you looked a little funny at me. To **Sofía Rodríguez Vásquez**, thanks for being a great person that I could always talk to, and not necessarily about science all the time. **Emelie Wallén Arzt**, you were the first lab-tech in the group, and did you straighten things up, organizing a lot of things around the lab! You are such a fun and great person to work with. To **Robin Hagblom**, thanks for helping me with genotypings and such in the lab, even though you didn't always have time. To **Juliane Schwaderer**, it was so fun going to the Nobel Lectures and Nobel Museum together, and when you accompanied me in the gym hitting the "killerbells". Thanks to all other past students of our group, **Adnan Popaja**, **Johan Holtby**, **Neshmil Rada** and **Aileen Bleisch**.

Thanks to **Serena Barilla**, you are such a sweet person, always caring and asking how things are going. To other past and present lunch buddies. **Marco Giudici**, **Saioa Goñi**, it was so much fun having you here. **Rodrigo Lozano**, **Sandra Scharaw** and **Ana Amaral**, you are the newest additions to the company around the lunch table, and so far you are doing a great job adding to all the serious discussion that we have! Oh, by the way, **Gwladys**, **Agustín**, **Hafdís**, **Irene**, **Peter** and **Serena**, thanks for allowing me to scream at you from time to time, I love teaching Bodycombat to you – you are all awesome fighters!

Many thanks to **Björn Rozell** and **Raoul Kuiper** for your great pathological consultations, I learn something new every time I sit down with you.

Thanks to all my other co-authors. To **Antti Koskela**, **Juha Tuukkanen** and **Claes Ohlsson** for great collaboration and support in Paper I. To **Karin Pernold**, **Thibaud J.C Richard**, **Fred W. Van Leeuwen**, **Nico P. Dantuma**, **Peter Damberg**, **Kjell Hultenby**, **Brun Ulfhake** and **Enrico Mugnaini** for collaboration and making Paper II possible. To **Tak-Heun Kim**, **Hwajung Choi** and **Eui-Sic Cho** for initiating the collaboration for Paper III. To **Pingnan Xiao** and **Hong Qian** for collaboration and great discussions resulting in Paper IV.

Great thanks to my other scientific collaborators. **Åsa-Lena Dackland**, for helping me with FACS analysis experiments, sometimes until very late in the evenings. **Åsa Bergström**, for helping me with various technical things around the department. Great thanks to **Moustapha Hassan** for running an excellent animal facility. We may not agree on things every time, but you always put the research first and help us solve the problems at hand. Thanks to **Mikael Zmarzlak** for being such a delight to work with and talk to in the animal facility. I would also like to thank **Angelica Eriksson**, **Jessica Åkerlund**, **Åsa Eriksson**, **Diana Lindroth** and all the other staff in the animal facility for their work and help with the mice.

I would also like to thank all the staff at the administrative and IT-unit at the department, especially **Monica Ahlberg**, **Marie Franzén**, **Lena Magnell** and **Vivian Saucedo Hildebrand** for all your great help and making everything so much easier. Many thanks also

to the service unit for all your great work, and special thanks to **Inger Moge** and **Johan Dethlefsen**, you two always have the answer to whatever question I come with.

Thanks to the **Progeria Research Foundation** for organizing very stimulating research meetings, and a special thanks to all the **progeria children** for showing us the value in our research.

Warm thanks to my wonderful friends. **Isabella Habijan**, we got to know each other through Campushallen in Linköping, for which I am forever grateful. We have spent countless of hours together in the gym over the past 12 years, and I look forward to having the opportunity to do it more frequently again soon. You are such a great friend, one of the warmest and most engaging persons I know. It is a comfort knowing that I can always talk to you, no matter the issue or reason. **Cecilia Esterling**, you I also got to know through the gym, back in the day when you used to attend my Bodycombat classes and kick and scream for all that you were worth. That is, until you took the plunge and also started teaching. And I have so amazingly fun when we team-teach classes, what a rush! Since the first time we met you have become a very dear friend of mine. **Anna Wallgren**, you were first my pole dance teacher, and then you became a great friend, and I miss hanging out with you every week. You have taught me some pretty amazing things on the pole over the years, and even though I'm not there right now, I'm really looking forward to the day I get to train for you again. You are such an inspiration in all your power, completely my cup of tea! **Sofia Palmqvist**, you are a really sweet and caring person, always having something interesting to discuss. It was so fun having you accompany us in Spain last year, and I hope that you will join us again for our next trip!

To my dear family, my mother **Barbro Pettersson** and my brother **Daniel Strandgren**, thank you for always believing in me. You are both so intelligent and curious, no wonder I have always wanted to know how everything works! I also have very special thanks to my cousin, **Jenny Lithén**, you are indeed my sister-in-heart. You are such an amazing person, and I have always looked up to you, wanting to be like you. Always have, always will. I love you all very much. I would also like to direct great thanks to the **Berg's**: **Ingrid**, **Håkan**, **Johan**, **Rickard** and **Olof**. Thank you for welcoming me into your family with open arms, and for all the fun times and interesting discussions we have had over the years. And thank you for giving Martin the upbringing that made him become the amazing person that he is.

To my cat, **Busan**. You were my first love, my first baby. Loosing you devastated me. I pray every day that you somehow will come back to me. And when you do, I will know it is you.

To my husband, **Martin Strandgren**. You are the best thing that has ever happened to me, and you make me the happiest person in the world. Thank you for always believing in me and supporting me, for comforting me when I am sad and for giving my life so much joy. Thank you for loving me, I wish I could express how much I love you. Thank you for being you. To my daughter, **Isabella Strandgren**. You are the happiest little person I know, and you are going to be a great big sister. Watching you develop brings me so much joy all the time. I can't even begin telling you how much I love you, but I will do my best everyday. I love you!

This work was mainly supported by grants from the Karolinska Institutet KID funding, the Progeria Research Foundation, the Swedish Research Council, and the Center for Innovative Medicine.

8 REFERENCES

Abad, V., J.L. Meyers, M. Weise, R.I. Gafni, K.M. Barnes, O. Nilsson, J.D. Bacher, and J. Baron. 2002. The role of the resting zone in growth plate chondrogenesis. *Endocrinology* 143:1851-1857.

Alford, A.I., K.M. Kozloff, and K.D. Hankenson. 2015. Extracellular matrix networks in bone remodeling. *Int J Biochem Cell Biol* 65:20-31.

Bonewald, L.F. 2011. The amazing osteocyte. *J Bone Miner Res* 26:229-238.

Bonewald, L.F., and M.L. Johnson. 2008. Osteocytes, mechanosensing and Wnt signaling. *Bone* 42:606-615.

Bridger, J.M., and I.R. Kill. 2004. Aging of Hutchinson-Gilford progeria syndrome fibroblasts is characterised by hyperproliferation and increased apoptosis. *Exp Gerontol* 39:717-724.

Burke, B., and C.L. Stewart. 2002. Life at the edge: the nuclear envelope and human disease. *Nat Rev Mol Cell Biol* 3:575-585.

Burke, B., and C.L. Stewart. 2006. The laminopathies: the functional architecture of the nucleus and its contribution to disease. *Annu Rev Genomics Hum Genet* 7:369-405.

Cao, K., C.D. Blair, D.A. Faddah, J.E. Kieckhaefer, M. Olive, M.R. Erdos, E.G. Nabel, and F.S. Collins. 2011a. Progerin and telomere dysfunction collaborate to trigger cellular senescence in normal human fibroblasts. *J Clin Invest* 121:2833-2844.

Cao, K., B.C. Capell, M.R. Erdos, K. Djabali, and F.S. Collins. 2007. A lamin A protein isoform overexpressed in Hutchinson-Gilford progeria syndrome interferes with mitosis in progeria and normal cells. *Proc Natl Acad Sci U S A* 104:4949-4954.

Cao, K., J.J. Graziotto, C.D. Blair, J.R. Mazzulli, M.R. Erdos, D. Krainc, and F.S. Collins. 2011b. Rapamycin reverses cellular phenotypes and enhances mutant protein clearance in Hutchinson-Gilford progeria syndrome cells. *Sci Transl Med* 3:89ra58.

Capell, B.C., and F.S. Collins. 2006. Human laminopathies: nuclei gone genetically awry. *Nat Rev Genet* 7:940-952.

Capell, B.C., M.R. Erdos, J.P. Madigan, J.J. Fiordalisi, R. Varga, K.N. Conneely, L.B. Gordon, C.J. Der, A.D. Cox, and F.S. Collins. 2005. Inhibiting farnesylation of progerin prevents the characteristic nuclear blebbing of Hutchinson-Gilford progeria syndrome. *Proc Natl Acad Sci U S A* 102:12879-12884.

Capell, B.C., M. Olive, M.R. Erdos, K. Cao, D.A. Faddah, U.L. Tavarez, K.N. Conneely, X. Qu, H. San, S.K. Ganesh, X. Chen, H. Avallone, F.D. Kolodgie, R. Virmani, E.G. Nabel, and F.S. Collins. 2008. A farnesyltransferase inhibitor prevents both the onset and late progression of cardiovascular disease in a progeria mouse model. *Proc Natl Acad Sci U S A* 105:15902-15907.

Chan, J., S.N. Waddington, K. O'Donoghue, H. Kurata, P.V. Guillot, C. Gotherstrom, M. Themis, J.E. Morgan, and N.M. Fisk. 2007. Widespread distribution and muscle differentiation of human fetal mesenchymal stem cells after intrauterine transplantation in dystrophic mdx mouse. *Stem Cells* 25:875-884.

Chen, J., M.B. Kelz, G. Zeng, N. Sakai, C. Steffen, P.E. Shockett, M.R. Picciotto, R.S. Duman, and E.J. Nestler. 1998. Transgenic animals with inducible, targeted gene expression in brain. *Mol Pharmacol* 54:495-503.

Chen, Z.J., W.P. Wang, Y.C. Chen, J.Y. Wang, W.H. Lin, L.A. Tai, G.G. Liou, C.S. Yang, and Y.H. Chi. 2014. Dysregulated interactions between lamin A and SUN1 induce abnormalities in the nuclear envelope and endoplasmic reticulum in progeric laminopathies. *J Cell Sci* 127:1792-1804.

Chung, U.I., E. Schipani, A.P. McMahon, and H.M. Kronenberg. 2001. Indian hedgehog couples chondrogenesis to osteogenesis in endochondral bone development. *J Clin Invest* 107:295-304.

Clements, L., S. Manilal, D.R. Love, and G.E. Morris. 2000. Direct interaction between emerin and lamin A. *Biochem Biophys Res Commun* 267:709-714.

Crisp, M., Q. Liu, K. Roux, J.B. Rattner, C. Shanahan, B. Burke, P.D. Stahl, and D. Hodzic. 2006. Coupling of the nucleus and cytoplasm: role of the LINC complex. *J Cell Biol* 172:41-53.

Dallas, S.L., and L.F. Bonewald. 2010. Dynamics of the transition from osteoblast to osteocyte. *Ann N Y Acad Sci* 1192:437-443.

De Sandre-Giovannoli, A., R. Bernard, P. Cau, C. Navarro, J. Amiel, I. Boccaccio, S. Lyonnet, C.L. Stewart, A. Munnich, M. Le Merrer, and N. Levy. 2003. Lamin a truncation in Hutchinson-Gilford progeria. *Science* 300:2055.

DeBusk, F.L. 1972. The Hutchinson-Gilford progeria syndrome. Report of 4 cases and review of the literature. *J Pediatr* 80:697-724.

Dechat, T., S.A. Adam, P. Taimen, T. Shimi, and R.D. Goldman. 2010. Nuclear lamins. *Cold Spring Harb Perspect Biol* 2:a000547.

Dechat, T., B. Korbei, O.A. Vaughan, S. Vlcek, C.J. Hutchison, and R. Foisner. 2000. Lamina-associated polypeptide 2alpha binds intranuclear A-type lamins. *J Cell Sci* 113 Pt 19:3473-3484.

Dechat, T., K. Pfleghaar, K. Sengupta, T. Shimi, D.K. Shumaker, L. Solimando, and R.D. Goldman. 2008. Nuclear lamins: major factors in the structural organization and function of the nucleus and chromatin. *Genes Dev* 22:832-853.

Dechat, T., T. Shimi, S.A. Adam, A.E. Rusinol, D.A. Andres, H.P. Spielmann, M.S. Sinensky, and R.D. Goldman. 2007. Alterations in mitosis and cell cycle progression caused by a mutant lamin A known to accelerate human aging. *Proc Natl Acad Sci U S A* 104:4955-4960.

Devine, S.M., C. Cobbs, M. Jennings, A. Bartholomew, and R. Hoffman. 2003. Mesenchymal stem cells distribute to a wide range of tissues following systemic infusion into nonhuman primates. *Blood* 101:2999-3001.

Dezawa, M., H. Ishikawa, Y. Itokazu, T. Yoshihara, M. Hoshino, S. Takeda, C. Ide, and Y. Nabeshima. 2005. Bone marrow stromal cells generate muscle cells and repair muscle degeneration. *Science* 309:314-317.

Eriksson, M., W.T. Brown, L.B. Gordon, M.W. Glynn, J. Singer, L. Scott, M.R. Erdos, C.M. Robbins, T.Y. Moses, P. Berglund, A. Dutra, E. Pak, S. Durkin, A.B. Csoka, M. Boehnke, T.W. Glover, and F.S. Collins. 2003. Recurrent de novo point mutations in lamin A cause Hutchinson-Gilford progeria syndrome. *Nature* 423:293-298.

Fisher, D.Z., N. Chaudhary, and G. Blobel. 1986. cDNA sequencing of nuclear lamins A and C reveals primary and secondary structural homology to intermediate filament proteins. *Proc Natl Acad Sci U S A* 83:6450-6454.

Foisner, R., and L. Gerace. 1993. Integral membrane proteins of the nuclear envelope interact with lamins and chromosomes, and binding is modulated by mitotic phosphorylation. *Cell* 73:1267-1279.

Fong, L.G., D. Frost, M. Meta, X. Qiao, S.H. Yang, C. Coffinier, and S.G. Young. 2006. A protein farnesyltransferase inhibitor ameliorates disease in a mouse model of progeria. *Science* 311:1621-1623.

Gabriel, D., L.B. Gordon, and K. Djabali. 2016. Temsirolimus Partially Rescues the Hutchinson-Gilford Progeria Cellular Phenotype. *PLoS One* 11:e0168988.

Gabriel, D., D. Roedl, L.B. Gordon, and K. Djabali. 2015. Sulforaphane enhances progerin clearance in Hutchinson-Gilford progeria fibroblasts. *Aging Cell* 14:78-91.

Gerber, H.P., T.H. Vu, A.M. Ryan, J. Kowalski, Z. Werb, and N. Ferrara. 1999. VEGF couples hypertrophic cartilage remodeling, ossification and angiogenesis during endochondral bone formation. *Nat Med* 5:623-628.

Gilford, H. 1897. On a Condition of Mixed Premature and Immature Development. *Med Chir Trans* 80:17-46 25.

Glynn, M.W., and T.W. Glover. 2005. Incomplete processing of mutant lamin A in Hutchinson-Gilford progeria leads to nuclear abnormalities, which are reversed by farnesyltransferase inhibition. *Hum Mol Genet* 14:2959-2969.

Goldman, R.D., Y. Gruenbaum, R.D. Moir, D.K. Shumaker, and T.P. Spann. 2002. Nuclear lamins: building blocks of nuclear architecture. *Genes Dev* 16:533-547.

Goldman, R.D., D.K. Shumaker, M.R. Erdos, M. Eriksson, A.E. Goldman, L.B. Gordon, Y. Gruenbaum, S. Khuon, M. Mendez, R. Varga, and F.S. Collins. 2004. Accumulation of mutant lamin A causes progressive changes in nuclear architecture in Hutchinson-Gilford progeria syndrome. *Proc Natl Acad Sci U S A* 101:8963-8968.

Gordon, C.M., L.B. Gordon, B.D. Snyder, A. Nazarian, N. Quinn, S. Huh, A. Giobbie-Hurder, D. Neuberg, R. Cleveland, M. Kleinman, D.T. Miller, and M.W. Kieran. 2011. Hutchinson-Gilford progeria is a skeletal dysplasia. *J Bone Miner Res* 26:1670-1679.

Gordon, L.B. 2016. PRF by the Numbers. *Progeria Research Foundation [Internet]*. Accessed 25 January, 2017.

Gordon, L.B., M.E. Kleinman, J. Massaro, R.B. D'Agostino, Sr., H. Shappell, M. Gerhard-Herman, L.B. Smoot, C.M. Gordon, R.H. Cleveland, A. Nazarian, B.D. Snyder, N.J. Ullrich, V.M. Silvera, M.G. Liang, N. Quinn, D.T. Miller, S.Y. Huh, A.A. Dowton, K. Littlefield, M.M. Greer, and M.W. Kieran. 2016. Clinical Trial of the Protein Farnesylation Inhibitors Lonafarnib, Pravastatin, and Zoledronic Acid in Children With Hutchinson-Gilford Progeria Syndrome. *Circulation* 134:114-125.

Gordon, L.B., M.E. Kleinman, D.T. Miller, D.S. Neuberg, A. Giobbie-Hurder, M. Gerhard-Herman, L.B. Smoot, C.M. Gordon, R. Cleveland, B.D. Snyder, B. Fligor, W.R. Bishop, P. Statkevich, A. Regen, A. Sonis, S. Riley, C. Ploski, A. Correia, N. Quinn, N.J. Ullrich, A. Nazarian, M.G. Liang, S.Y. Huh, A. Schwartzman, and M.W. Kieran. 2012. Clinical trial of a farnesyltransferase inhibitor in children with Hutchinson-Gilford progeria syndrome. *Proc Natl Acad Sci U S A* 109:16666-16671.

Gordon, L.B., J. Massaro, R.B. D'Agostino, Sr., S.E. Campbell, J. Brazier, W.T. Brown, M.E. Kleinman, M.W. Kieran, and C. Progeria Clinical Trials. 2014a. Impact of farnesylation inhibitors on survival in Hutchinson-Gilford progeria syndrome. *Circulation* 130:27-34.

Gordon, L.B., K.M. McCarten, A. Giobbie-Hurder, J.T. Machan, S.E. Campbell, S.D. Berns, and M.W. Kieran. 2007. Disease progression in Hutchinson-Gilford progeria syndrome: impact on growth and development. *Pediatrics* 120:824-833.

Gordon, L.B., F.G. Rothman, C. López-Otín, and T. Misteli. 2014b. Progeria: a paradigm for translational medicine. *Cell* 156:400-407.

Gossen, M., and H. Bujard. 1992. Tight control of gene expression in mammalian cells by tetracycline-responsive promoters. *Proc Natl Acad Sci U S A* 89:5547-5551.

Gudise, S., R.A. Figueroa, R. Lindberg, V. Larsson, and E. Hallberg. 2011. Samp1 is functionally associated with the LINC complex and A-type lamina networks. *J Cell Sci* 124:2077-2085.

Guillot, P.V., O. Abass, J.H. Bassett, S.J. Shefelbine, G. Bou-Gharios, J. Chan, H. Kurata, G.R. Williams, J. Polak, and N.M. Fisk. 2008. Intrauterine transplantation of human fetal mesenchymal stem cells from first-trimester blood repairs bone and reduces fractures in osteogenesis imperfecta mice. *Blood* 111:1717-1725.

Hennekam, R.C. 2006. Hutchinson-Gilford progeria syndrome: review of the phenotype. *Am J Med Genet A* 140:2603-2624.

Horwitz, E.M., P.L. Gordon, W.K. Koo, J.C. Marx, M.D. Neel, R.Y. McNall, L. Muul, and T. Hofmann. 2002. Isolated allogeneic bone marrow-derived mesenchymal cells engraft and stimulate growth in children with osteogenesis imperfecta: Implications for cell therapy of bone. *Proc Natl Acad Sci U S A* 99:8932-8937.

Horwitz, E.M., D.J. Prockop, L.A. Fitzpatrick, W.W. Koo, P.L. Gordon, M. Neel, M. Sussman, P. Orchard, J.C. Marx, R.E. Pyeritz, and M.K. Brenner. 1999. Transplantability and therapeutic effects of bone marrow-derived mesenchymal cells in children with osteogenesis imperfecta. *Nat Med* 5:309-313.

Horwitz, E.M., D.J. Prockop, P.L. Gordon, W.W. Koo, L.A. Fitzpatrick, M.D. Neel, M.E. McCarville, P.J. Orchard, R.E. Pyeritz, and M.K. Brenner. 2001. Clinical responses to bone marrow transplantation in children with severe osteogenesis imperfecta. *Blood* 97:1227-1231.

Hutchinson, J. 1886. Congenital Absence of Hair and Mammary Glands with Atrophic Condition of the Skin and its Appendages, in a Boy whose Mother had been almost wholly Bald from Alopecia Areata from the age of Six. *Med Chir Trans* 69:473-477.

Ibrahim, M.X., V.I. Sayin, M.K. Akula, M. Liu, L.G. Fong, S.G. Young, and M.O. Bergo. 2013. Targeting isoprenylcysteine methylation ameliorates disease in a mouse model of progeria. *Science* 340:1330-1333.

Kieran, M.W., L. Gordon, and M. Kleinman. 2007. New approaches to progeria. *Pediatrics* 120:834-841.

Kolb, T., K. Maass, M. Hergt, U. Aebi, and H. Herrmann. 2011. Lamin A and lamin C form homodimers and coexist in higher complex forms both in the nucleoplasmic fraction and in the lamina of cultured human cells. *Nucleus* 2:425-433.

Kronenberg, H.M. 2003. Developmental regulation of the growth plate. *Nature* 423:332-336.

Kubben, N., W. Zhang, L. Wang, T.C. Voss, J. Yang, J. Qu, G.H. Liu, and T. Misteli. 2016. Repression of the Antioxidant NRF2 Pathway in Premature Aging. *Cell* 165:1361-1374.

Larrieu, D., S. Britton, M. Demir, R. Rodriguez, and S.P. Jackson. 2014. Chemical inhibition of NAT10 corrects defects of laminopathic cells. *Science* 344:527-532.

Lavasani, M., A.R. Robinson, A. Lu, M. Song, J.M. Feduska, B. Ahani, J.S. Tilstra, C.H. Feldman, P.D. Robbins, L.J. Niedernhofer, and J. Huard. 2012. Muscle-derived stem/progenitor cell dysfunction limits healthspan and lifespan in a murine progeria model. *Nat Commun* 3:608.

Lee, S.J., Y.S. Jung, M.H. Yoon, S.M. Kang, A.Y. Oh, J.H. Lee, S.Y. Jun, T.G. Woo, H.Y. Chun, S.K. Kim, K.J. Chung, H.Y. Lee, K. Lee, G. Jin, M.K. Na, N.C. Ha, C. Barcena, J.M. Freije, C. Lopez-Otin, G.Y. Song, and B.J. Park. 2016. Interruption of progerin-lamin A/C binding ameliorates Hutchinson-Gilford progeria syndrome phenotype. *J Clin Invest* 126:3879-3893.

Liechty, K.W., T.C. MacKenzie, A.F. Shaaban, A. Radu, A.M. Moseley, R. Deans, D.R. Marshak, and A.W. Flake. 2000. Human mesenchymal stem cells engraft and demonstrate site-specific differentiation after in utero transplantation in sheep. *Nat Med* 6:1282-1286.

Liu, B., S. Ghosh, X. Yang, H. Zheng, X. Liu, Z. Wang, G. Jin, B. Zheng, B.K. Kennedy, Y. Suh, M. Kaeberlein, K. Tryggvason, and Z. Zhou. 2012. Resveratrol rescues SIRT1-dependent adult stem cell decline and alleviates progeroid features in laminopathy-based progeria. *Cell Metab* 16:738-750.

Lombardi, M.L., D.E. Jaalouk, C.M. Shanahan, B. Burke, K.J. Roux, and J. Lammerding. 2011. The interaction between nesprins and sun proteins at the nuclear envelope is critical for force transmission between the nucleus and cytoskeleton. *J Biol Chem* 286:26743-26753.

Long, F., and D.M. Ornitz. 2013. Development of the endochondral skeleton. *Cold Spring Harb Perspect Biol* 5:a008334.

Lopez-Otin, C., M.A. Blasco, L. Partridge, M. Serrano, and G. Kroemer. 2013. The hallmarks of aging. *Cell* 153:1194-1217.

Machiels, B.M., A.H. Zorenc, J.M. Endert, H.J. Kuijpers, G.J. van Eys, F.C. Ramaekers, and J.L. Broers. 1996. An alternative splicing product of the lamin A/C gene lacks exon 10. *J Biol Chem* 271:9249-9253.

Makino, S., K. Fukuda, S. Miyoshi, F. Konishi, H. Kodama, J. Pan, M. Sano, T. Takahashi, S. Hori, H. Abe, J. Hata, A. Umezawa, and S. Ogawa. 1999. Cardiomyocytes can be generated from marrow stromal cells in vitro. *J Clin Invest* 103:697-705.

Mansour, A., G. Abou-Ezzi, E. Sitnicka, S.E. Jacobsen, A. Wakkach, and C. Blin-Wakkach. 2012. Osteoclasts promote the formation of hematopoietic stem cell niches in the bone marrow. *J Exp Med* 209:537-549.

Merideth, M.A., L.B. Gordon, S. Clauss, V. Sachdev, A.C. Smith, M.B. Perry, C.C. Brewer, C. Zalewski, H.J. Kim, B. Solomon, B.P. Brooks, L.H. Gerber, M.L. Turner, D.L. Domingo, T.C. Hart, J. Graf, J.C. Reynolds, A. Gropman, J.A. Yanovski, M. Gerhard-Herman, F.S. Collins, E.G. Nabel, R.O. Cannon, 3rd, W.A. Gahl, and W.J. Introne. 2008. Phenotype and course of Hutchinson-Gilford progeria syndrome. *N Engl J Med* 358:592-604.

Moir, R.D., and T.P. Spann. 2001. The structure and function of nuclear lamins: implications for disease. *Cell Mol Life Sci* 58:1748-1757.

Ono, N., W. Ono, T. Nagasawa, and H.M. Kronenberg. 2014. A subset of chondrogenic cells provides early mesenchymal progenitors in growing bones. *Nat Cell Biol* 16:1157-1167.

Osorio, F.G., C.L. Navarro, J. Cadinanos, I.C. Lopez-Mejia, P.M. Quiros, C. Bartoli, J. Rivera, J. Tazi, G. Guzman, I. Varela, D. Depetris, F. de Carlos, J. Cobo, V. Andres, A. De Sandre-Giovannoli, J.M. Freije, N. Levy, and C. Lopez-Otin. 2011. Splicing-directed therapy in a new mouse model of human accelerated aging. *Sci Transl Med* 3:106ra107.

Pittenger, M.F., A.M. Mackay, S.C. Beck, R.K. Jaiswal, R. Douglas, J.D. Mosca, M.A. Moorman, D.W. Simonetti, S. Craig, and D.R. Marshak. 1999. Multilineage potential of adult human mesenchymal stem cells. *Science* 284:143-147.

Progeria Research Foundation. 2016. Progeria Clinical Trials. *Progeria Research Foundation [Internet]*. Accessed 22 March, 2017.

Qian, H., A. Badaloni, F. Chiara, J. Stjernberg, N. Polisetti, K. Nihlberg, G.G. Consalez, and M. Sigvardsson. 2013. Molecular characterization of prospectively isolated multipotent mesenchymal progenitors provides new insight into the cellular identity of mesenchymal stem cells in mouse bone marrow. *Mol Cell Biol* 33:661-677.

Richards, S.A., J. Muter, P. Ritchie, G. Lattanzi, and C.J. Hutchison. 2011. The accumulation of un-repairable DNA damage in laminopathy progeria fibroblasts is caused by ROS generation and is prevented by treatment with N-acetyl cysteine. *Hum Mol Genet* 20:3997-4004.

Rober, R.A., K. Weber, and M. Osborn. 1989. Differential timing of nuclear lamin A/C expression in the various organs of the mouse embryo and the young animal: a developmental study. *Development* 105:365-378.

Rodriguez, S., F. Coppede, H. Sagelius, and M. Eriksson. 2009. Increased expression of the Hutchinson-Gilford progeria syndrome truncated lamin A transcript during cell aging. *Eur J Hum Genet* 17:928-937.

Rosengardten, Y., T. McKenna, D. Grochova, and M. Eriksson. 2011. Stem cell depletion in Hutchinson-Gilford progeria syndrome. *Aging Cell* 10:1011-1020.

Sagelius, H., Y. Rosengardten, M. Hanif, M.R. Erdos, B. Rozell, F.S. Collins, and M. Eriksson. 2008a. Targeted transgenic expression of the mutation causing Hutchinson-Gilford progeria syndrome leads to proliferative and degenerative epidermal disease. *J Cell Sci* 121:969-978.

Sagelius, H., Y. Rosengardten, E. Schmidt, C. Sonnabend, B. Rozell, and M. Eriksson. 2008b. Reversible phenotype in a mouse model of Hutchinson-Gilford progeria syndrome. *J Med Genet* 45:794-801.

Scaffidi, P., and T. Misteli. 2006. Lamin A-dependent nuclear defects in human aging. *Science* 312:1059-1063.

Scaffidi, P., and T. Misteli. 2008. Lamin A-dependent misregulation of adult stem cells associated with accelerated ageing. *Nat Cell Biol* 10:452-459.

Schmidt, E., O. Nilsson, A. Koskela, J. Tuukkanen, C. Ohlsson, B. Rozell, and M. Eriksson. 2012. Expression of the Hutchinson-Gilford progeria mutation during osteoblast development results in loss of osteocytes, irregular mineralization, and poor biomechanical properties. *J Biol Chem* 287:33512-33522.

Sinensky, M., K. Fantle, M. Trujillo, T. McLain, A. Kupfer, and M. Dalton. 1994. The processing pathway of prelamin A. *J Cell Sci* 107 (Pt 1):61-67.

Strandgren, C., H.A. Nasser, T. McKenna, A. Koskela, J. Tuukkanen, C. Ohlsson, B. Rozell, and M. Eriksson. 2015. Transgene silencing of the Hutchinson-Gilford progeria syndrome mutation results in a reversible bone phenotype, whereas resveratrol treatment does not show overall beneficial effects. *FASEB J* 29:3193-3205.

Stuurman, N., S. Heins, and U. Aebi. 1998. Nuclear lamins: their structure, assembly, and interactions. *J Struct Biol* 122:42-66.

Swift, J., I.L. Ivanovska, A. Buxboim, T. Harada, P.C. Dingal, J. Pinter, J.D. Pajerowski, K.R. Spinler, J.W. Shin, M. Tewari, F. Rehfeldt, D.W. Speicher, and D.E. Discher. 2013. Nuclear lamin-A scales with tissue stiffness and enhances matrix-directed differentiation. *Science* 341:1240104.

Thanisch, K., C. Song, D. Engelkamp, J. Koch, A. Wang, E. Hallberg, R. Foisner, H. Leonhardt, C.L. Stewart, B. Joffe, and I. Solovei. 2017. Nuclear envelope localization of LEMD2 is developmentally dynamic and lamin A/C dependent yet insufficient for heterochromatin tethering. *Differentiation* 94:58-70.

Toth, J.I., S.H. Yang, X. Qiao, A.P. Beigneux, M.H. Gelb, C.L. Moulson, J.H. Miner, S.G. Young, and L.G. Fong. 2005. Blocking protein farnesyltransferase improves nuclear shape in fibroblasts from humans with progeroid syndromes. *Proc Natl Acad Sci U S A* 102:12873-12878.

Turgay, Y., M. Eibauer, A.E. Goldman, T. Shimi, M. Khayat, K. Ben-Harush, A. Dubrovsky-Gaupp, K.T. Sapra, R.D. Goldman, and O. Medalia. 2017. The molecular architecture of lamins in somatic cells. *Nature* 543:261-264.

Uccelli, A., L. Moretta, and V. Pistoia. 2008. Mesenchymal stem cells in health and disease. *Nat Rev Immunol* 8:726-736.

Varela, I., S. Pereira, A.P. Ugalde, C.L. Navarro, M.F. Suarez, P. Cau, J. Cadinanos, F.G. Osorio, N. Foray, J. Cobo, F. de Carlos, N. Levy, J.M. Freije, and C. Lopez-Otin. 2008. Combined treatment with statins and aminobisphosphonates extends longevity in a mouse model of human premature aging. *Nat Med* 14:767-772.

Vidak, S., and R. Foisner. 2016. Molecular insights into the premature aging disease progeria. *Histochem Cell Biol* 145:401-417.

Xiong, Z.M., J.Y. Choi, K. Wang, H. Zhang, Z. Tariq, D. Wu, E. Ko, C. LaDana, H. Sesaki, and K. Cao. 2016. Methylene blue alleviates nuclear and mitochondrial abnormalities in progeria. *Aging Cell* 15:279-290.

Xiong, Z.M., C. LaDana, D. Wu, and K. Cao. 2013. An inhibitory role of progerin in the gene induction network of adipocyte differentiation from iPS cells. *Aging (Albany NY)* 5:288-303.

Yang, S.H., M.O. Bergo, J.I. Toth, X. Qiao, Y. Hu, S. Sandoval, M. Meta, P. Bendale, M.H. Gelb, S.G. Young, and L.G. Fong. 2005. Blocking protein farnesyltransferase improves nuclear blebbing in mouse fibroblasts with a targeted Hutchinson-Gilford progeria syndrome mutation. *Proc Natl Acad Sci U S A* 102:10291-10296.

Yang, S.H., M. Meta, X. Qiao, D. Frost, J. Bauch, C. Coffinier, S. Majumdar, M.O. Bergo, S.G. Young, and L.G. Fong. 2006. A farnesyltransferase inhibitor improves disease phenotypes in mice with a Hutchinson-Gilford progeria syndrome mutation. *J Clin Invest* 116:2115-2121.

Yang, S.H., X. Qiao, L.G. Fong, and S.G. Young. 2008. Treatment with a farnesyltransferase inhibitor improves survival in mice with a Hutchinson-Gilford progeria syndrome mutation. *Biochim Biophys Acta* 1781:36-39.

Young, S.G., M. Meta, S.H. Yang, and L.G. Fong. 2006. Prelamin A farnesylation and progeroid syndromes. *J Biol Chem* 281:39741-39745.

Zhang, H., Z.M. Xiong, and K. Cao. 2014. Mechanisms controlling the smooth muscle cell death in progeria via down-regulation of poly(ADP-ribose) polymerase 1. *Proc Natl Acad Sci U S A* 111:E2261-2270.

Zhang, J., Q. Lian, G. Zhu, F. Zhou, L. Sui, C. Tan, R.A. Mutalif, R. Navasankari, Y. Zhang, H.F. Tse, C.L. Stewart, and A. Colman. 2011. A human iPSC model of Hutchinson Gilford Progeria reveals vascular smooth muscle and mesenchymal stem cell defects. *Cell Stem Cell* 8:31-45.

Zhu, Z., T. Zheng, C.G. Lee, R.J. Homer, and J.A. Elias. 2002. Tetracycline-controlled transcriptional regulation systems: advances and application in transgenic animal modeling. *Semin Cell Dev Biol* 13:121-128.